Open access • Journal Article • DOI:10.1177/8755293020957350

Expanded Byrne model for evaluating seismic compression — Source link

Yusheng Jiang, Russell A. Green, Oliver-Denzil S. Taylor

Institutions: Virginia Tech, United States Army Corps of Engineers

Published on: 01 May 2021 - Earthquake Spectra (SAGE PublicationsSage UK: London, England)

Expanded Byrne Model for Evaluating Seismic Compression

by

Yusheng Jiang

Thesis submitted to the faculty of the Virginia Polytechnic Institute and State University in partial fulfillment of the requirements for the degree of

Master of Science
In
Civil Engineering

Russell A. Green
Adrian Rodriguez-Marek
Bernardo A. Castellanos

August 13, 2019
Blacksburg, VA

Keywords: Seismic compression; Byrne model; earthquake; settlement

Expanded Byrne Model for Evaluating Seismic Compression

Yusheng Jiang

ABSTRACT

The Byrne (1991) model was developed to predict excess pore water pressure for saturated sands under cyclic loading. However, the model can also be used to predict seismic compression in dry or partially saturated clean sands, which is the focus of this research. The original Byrne (1991) model has two primary limitations. One limitation is that calibration coefficients for the model have only been developed for clean sand, while seismic compression is a concern for a variety of soil types in engineering practice. Another limitation is that the existing calibration coefficients are solely correlated with soil relative density. This is in contrast to findings from studies performed over the last two decades that show various environmental and compositional factors, in addition to relative density, influence seismic compression behavior. To overcome these shortcomings and others the model was transformed to allow it to be implemented in "simplified" and "non-simplified" manners and systematic model calibration procedures were developed by means of MATLAB code. Both "simplified" and "non-simplified" variants of the model were used to analyze a site in Japan impacted by the 2007, M_w6.6 Niigata-ken Chuetsu-oki earthquake. The results from the analyses are in general accord with the post-earthquake field observations and highlight the utility and versatility of the models.

Expanded Byrne Model for Evaluating Seismic Compression

Yusheng Jiang

GENERAL AUDIENCE ABSTRACT

Earthquake shaking can cause compression of volume in soil, which may induce damage to various infrastructures. This phenomenon is known as seismic compression. Byrne (1991) proposed one model that can be used to evaluate the magnitude of seismic compression. However, this model has two significant limitations. One limitation is its coefficient expression is suitable for merely one soil type, while seismic compression is a concern for a variety of soil types in engineering practice. Another limitation is that the existing model coefficients are only correlated with soil density. This is in contrast to findings from research conducted over the last two decades that show many other environmental and compositional factors, in addition to soil density, affect the magnitude of seismic compression. To overcome these shortcomings and others the model was modified and calibrated, where mathematical transformations were performed for the model to allow it to be implemented in "simplified" and "non-simplified" calculation manners. Also, systematic model modification procedures were established by means of codes written by one software called MATLAB. Both the "simplified" and "non-simplified" calculation methods of the model were used to analyze a site in Japan impacted by an earthquake occurred in 2007, named Niigata-ken Chuetsu-oki Earthqauke. The results from the analyses are in general accord with the records obtained after the earthquake and highlight the utility and versatility of the modified models.

Acknowledgements

I extend a special mention to my advisor Dr. Russell A. Green who assisted in the topic selection and helped a lot in research direction instruction. His advice, guidance, support, and encouragement throughout the course of all my graduate studies are gratefully acknowledged. The laboratory work undertaken by researchers from UCLA: Drs. Jonathan P. Stewart, Daniel H. Whang, Pendo Duku, and Eric Yee was very valuable to this research. Additionally, Drs. Jonathan Stewart, Pengfei Wang, and Tadahiro Kishida assisted in obtaining the ground motions used in the analysis of the case history. This study is based on work supported in part by the US Army Engineer Research and Development Center (ERDC) Grant W912HZ-13-C-0035 and in part by the U.S. National Science Foundation (NSF) grants CMMI-1030564, CMMI-1435494, CMMI-1724575, and CMMI-1825189. The authors gratefully acknowledge this support. However, any opinions, findings, and conclusions expressed in this thesis are those of the author and do not necessarily reflect the views of ERDC, NSF, or others.

Table of Contents

List of Tables

List of Figures

Chapter 1: Introduction

1.1 Problem Statement

The objective of the study presented herein is to expand the Byrne cycle shear-volume strain coupling model to accurately predict seismic compression for several soil types and to provide both simplified and non-simplified versions of the model. Achievement of this objective will further the overall goal of providing a framework that can accurately evaluate seismic compression, that is scalable based on available data and the importance of the project, and that overcomes some of the complexity issues with existing models in implementing non-simplified procedures. The Byrne (1991) model developed to predict excess pore water pressure for saturated sands under cyclic loading. However, the model can also be used to predict seismic compression in dry or partially saturated clean sands, which is the focus of this research. The original Byrne (1991) model has two primary limitations. One limitation is that calibration coefficients for the model have only been developed for clean sand, while seismic compression is a concern for a variety of soil types in engineering practice. Another limitation is that the model coefficients are solely correlated with soil relative density. However, recent experimental findings indicated that, in addition to relative density, factors such as degree of saturation, overburden pressure, and fine content, also impact soil seismic compression behaviors. Since none of these factors were considered in the Byrne (1991) model, plus a greatly enlarged laboratory test database is now available for more soil types, systematic model calibration procedures were developed by means of MATLAB code.

1.2 Organization

This thesis is organized into three chapters and four appendices (A-D). The second chapter is a manuscript that will be submitted as a technical paper to a recognized journal in the field of geotechnical and/or earthquake engineering. The third chapter of this thesis summarizes the primary performed work, main findings, and recommendations for future research. The back matter of this thesis contains four appendices which offer further detail on: the Byrne (1991) model equation derivations, methods of obtaining regressed coefficients, Byrne model calibration based on the UCLA models, and the related MATLAB code used in the study.

1.3 Attribution

The manuscript contained in Chapter 2 entitled: “Expanded Byrne Model for Evaluating Seismic Compression” authored by Yusheng Jiang is expected to be published as a technical paper. The contributing co-author and his primary role pertaining to this paper is provided below:

Russell A. Green, Ph.D., Department of Civil and Environmental Engineering, Virginia Tech, Blacksburg, Virginia, U.S.A

- Research Advisor to the lead author, who provided significant oversight and guidance during all phases of this research. Dr. Green is also credited for establishing the adopted approaches for computing the number of equivalent shear cycles, stress reduction coefficient, and two-dimensional shaking correction factor within this study.

Chapter 2: Expanded Byrne Model for Evaluating Seismic Compression

2.1 Abstract

Seismic compression is the accrual of contractive volumetric strain in unsaturated or partially saturated sandy soils during earthquake shaking and has caused significant distress to overlying and nearby structures. The phenomenon can be well-characterized by load-dependent, interaction macro-level fatigue theories. Towards this end, the Byrne cyclic shear-volume strain coupling model is expanded and calibrated for evaluating seismic compression for several soil types. Additionally, the model was transformed to allow it to be implemented in a "simplified" manner, in addition to the original "non-simplified" formulation. Both implementation approaches are used to analyze a site in Japan impacted by the 2007, M_w6.6 Niigata-ken Chuetsu-oki earthquake. The results from the analyses are in general accord with the post-earthquake field observations and highlight the utility and versatility of the models.

2.2 Introduction

Seismic compression is the accrual of contractive volumetric strain in unsaturated or partially saturated sandy soils during earthquake shaking (i.e., vibration-induced settlement) (Stewart et al. 2004a). Seismic compression has occurred in several earthquakes and can significantly distress overlying and nearby structures (e.g., Slosson 1975; Siddharthan and El-Gamal 1996; Stewart et al. 2004a). Adopting the terminology used for liquefaction triggering procedures, with slight modification, seismic compression evaluation procedures can be broadly classified as "simplified" and "non-simplified." In the context used herein, simplified approaches use relatively simple ground motion parameterization to characterize the seismic demand (e.g., effective shear strain, γ_{eff}, and number of equivalent strain cycles, $n_{eq\gamma}$), while non-simplified procedures use more detailed characterization of seismic demand (e.g., shear strain, γ, time histories computed using numerical site response analyses).

The majority of the seismic compression evaluation procedures proposed to date are simplified procedures, with an evolved form of the Tokimatsu and Seed (1987) procedure defining the state-of-practice. Consistent with how simplified procedures are defined, the Tokimatsu and Seed (1987) procedure uses a magnitude (M) 7.5 as a reference scenario and quantifies the seismic demand in terms of γ_{eff} and $n_{eq\gamma}$. Using these seismic demand parameters, volumetric strain is then estimated using correlations derived from the observed trends in laboratory test data.

To the authors' knowledge, Finn and Byrne (1976) were the first to propose a non-simplified approach for evaluating seismic compression. In their procedure the seismic demand is quantified in terms of shear strain time histories acting on horizontal planes at various depths within the soil profile, computed by numerical site response analyses. Increments in volumetric strain are then computed using a model proposed by Martin et al. (1975) that relates shear and volumetric strains. As discussed in Green and Lee (2006) and Lasley et al. (2016a), the Martin et al. (1975) model is a load-dependent, interaction macro-level fatigue model, as is the subsequently proposed variant by Byrne (1991) (i.e., the nature of the accumulation of volumetric strain is a function of the amplitude of the load and is influenced by previous loading, e.g., Kaechele 1963). Both the Martin et al. (1975) model and the Byrne (1991) variant were calibrated to the same clean sand dataset used by Tokimatsu and Seed (1987). It is difficult to state what defines the state-of-practice of non-simplified seismic compression evaluation procedures because they have not been widely adopted by practice. However, the non-simplified procedure by Lasley et al. (2016a) is the latest one to have been proposed, at least to the authors' knowledge.

The main advantage of non-simplified procedures is that they allow for the use of a more detailed characterization of the seismic demand at all depths in the profile. Most notably, this allows the variation in induced shear strains over the duration of shaking to be accounted for, which influences the resulting volumetric strain in materials that exhibit load-dependent, interaction fatigue behavior. Because performing site response analyses needed for implementing non-simplified procedures has become state-of-practice in many places, non-simplified procedures are a viable option for predicting seismic compression in today's practice. The disadvantage of using non-simplified procedures is that they require more effort to implement, to include a more-detailed characterization of the site being analyzed, selection of appropriate input ground motions for the site response analysis, and the complexity of implementing the procedure itself.

The objective of the study presented herein is to expand the Byrne cyclic shear-volume strain coupling model to accurately predict seismic compression for several soil types and to provide both simplified and non-simplified versions of the model. Achievement of this objective will further the overall goal of providing a framework that can accurately evaluate seismic compression, that is scalable based on available data and the importance of the project, and that overcomes some of the complexity issues with existing models in implementing non-simplified procedures.

In the following, additional information is provided regarding simplified and non-simplified seismic compression evaluation procedures. Next, the Byrne model is expanded to better account for observed volumetric strain behavior in laboratory test data and is calibrated for different soil types using data from literature and using published simplified procedures. The proposed simplified and non-simplified variants of the expanded Byrne model are then used to

analyze a well-documented case history from the 2007, M_w6.6 Niigata-ken Chuetsu-oki earthquake, with the results discussed in the context of the utility and versatility of the models.

2.3 Background

2.3.1 Simplified Procedures

The first simplified seismic compression procedure was proposed by Seed and Silver (1972). In this procedure, the shear strain time histories acting on horizontal planes at various depths within in a profile are computed using a numerical site response analysis, from which both γ_{eff} and $n_{eq\gamma}$ are computed as a function of depth within the profile. Drained cyclic direct simple shear tests performed on samples representative of in-situ soil and state are performed to develop relationships among γ_{eff}, relative density (Dr), $n_{eq\gamma}$, and volumetric strain (ε_v), where Seed and Silver (1972) present such relationships for Crystal Silica No. 20 sand (i.e., a uniform angular quartz sand having D_{10} ~ 0.5 mm and a uniformity coefficient of ~1.5; D_{10} is the effective soil particle diameter corresponding to 10% passing on the grain size distribution curve).

Tokimatsu and Seed (1987) furthered the simplified framework put forward by Seed and Silver (1972) in several ways. In the Tokimatsu and Seed (1987) procedure, γ_{eff} is estimated using an expression that was derived similarly to the one used to compute Cyclic Stress Ratio (CSR) in simplified liquefaction evaluation procedures:

$$\gamma_{eff} = \frac{\tau_{av}}{G_{\gamma_{eff}}} \approx \frac{0.65 \cdot \frac{a_{max}}{g} \cdot \sigma_v \cdot r_d}{G_{max} \cdot \left(\frac{G}{G_{max}}\right)_{\gamma_{eff}}} \quad (1)$$

where: τ_{av} is the average cyclic stress imposed on the soil at given depth in the profile over the duration of strong ground shaking; $G_{\gamma eff}$ is the secant shear modulus corresponding to γ_{eff}; a_{max} is the peak horizontal ground acceleration at the surface of the soil profile; g is the acceleration due to gravity in the same units as a_{max}; σ_v is the total vertical stress at the depth of interest; r_d is the dimensionless depth-stress reduction factor that accounts for the non-linear response of the profile during earthquake shaking; G_{max} is the small strain ($\gamma < 10^{-4}$%) secant shear modulus in the same units as σ_v; and $(G/G_{max})_{\gamma eff}$ is the ratio of $G_{\gamma eff}$ and G_{max}. Because γ_{eff} is a function of a $G_{\gamma eff}$ (or $G_{max} \cdot (G/G_{max})_{\gamma eff}$) which in turn is a function of γ_{eff}, Eq. (1) needs to be solved iteratively or using the chart solution proposed by Tokimatsu and Seed (1987), or similar ones.

The resulting γ_{eff} value is used in conjunction with $n_{eq\gamma}$, which is estimated using a correlation that relates $n_{eq\gamma}$ to M, a_{max}, site-to-source distance, and/or other parameters, to define the seismic demand imposed on the soil at a given depth in the profile. Estimation of γ_{eff} and $n_{eq\gamma}$ using this

approach avoids the need to perform numerical site response analyses and the associated efforts of performing detailed site characterization and selecting appropriate input ground motions for the site response analysis.

Using the laboratory data for Crystal Silica Sand No. 2 from Silver and Seed (1971) and Seed and Silver (1972), Tokimatsu and Seed (1987) developed the relationships shown in Figure 1, one relating ε_v for $n_{eq\gamma} = 15$ (i.e., $\varepsilon_{v,15}$), relative density (Dr) of the soil, and γ_{eff}, and the other relating the volumetric strain ratio (C_N), which is the ratio ε_v for a given value of $n_{eq\gamma}$ to $\varepsilon_{v,15}$ (i.e., $C_N = \varepsilon_{v,n}/\varepsilon_{v,15}$), and $n_{eq\gamma}$. The basis for using $n_{eq\gamma} = 15$ as a reference condition was likely to provide consistency with the simplified liquefaction evaluation procedures which use M7.5 as the reference condition, with early correlations relating M and number of equivalent stress cycles ($n_{eq\tau}$) predicting $n_{eq\tau} = 15$ for M7.5 (e.g., Seed et al. 1975).

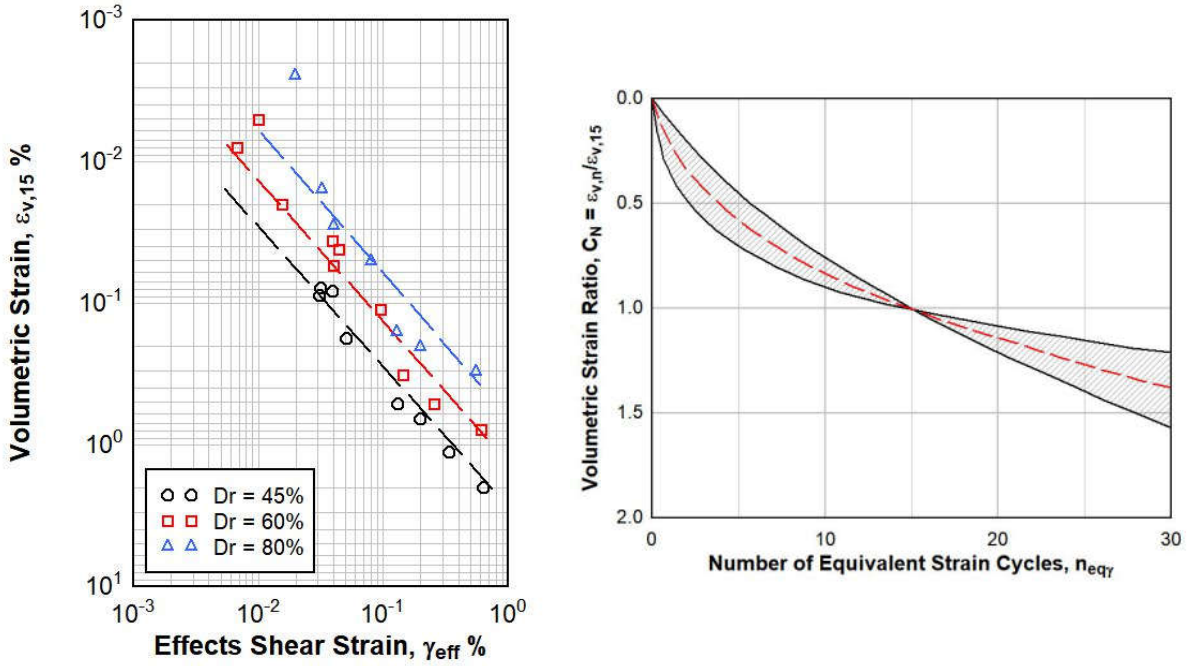

(a) (b)

Figure 1: Relationships derived from laboratory test data from Silver and Seed (1971): (a) relationship between $\varepsilon_{v,15}$ and γ_{eff}; and (b) relationship between C_N and $n_{eq\gamma}$. (after Tokimatsu and Seed 1987)

Several laboratory studies have built on the Tokimatsu and Seed (1987) framework by examining the effect of saturation (S), Dr, fines content (FC), mineralogy, fabric, overconsolidation ratio (OCR), plasticity index (PI), effective overburden stress (σ'_v), and multidirectional shaking on seismic compression (e.g., Pyke et al. 1975; Chu and Vucetic 1992; Whang 2001; Hsu and Vucetic 2004; Stewart et al. 2004a; Whang et al. 2004; Sawada et al. 2006; Duku et al. 2008; Yee et al. 2014; Carter et al. 2016). Also, additional studies have developed revised number of equivalent cycle correlations (e.g., Liu et al. 2001; Hancock and Bommer 2005; Green and Lee 2006; Stafford and Bommer 2009; Lasley et al. 2017; Lee and Green 2017). As a result, the overall simplified framework proposed by Tokimatsu and Seed

(1987) has evolved and thus still defines the state-of-practice for evaluating seismic compression.

As part of the evolution of the Tokimatsu and Seed (1987) procedure, Duku et al. (2008) performed extensive laboratory tests on 16 different types of clean sands and proposed the following relationships for $\varepsilon_{v,15}$ and C_N:

$$\varepsilon_{v,15} = a \cdot \left(\gamma_{eff} - \gamma_{tv}\right)^b \quad (2a)$$

$$C_N = R \cdot \ln\left(n_{eq\gamma}\right) + c \quad (2b)$$

where a and b are material-specific constants; γ_{tv} is the volumetric threshold strain (0.01 – 0.03% for sand; Hsu and Vucetic 2004); R is the slope of the line fit through C_N vs. $\log(n_{eq\gamma})$ data; and c = 1-[ln(15)·R]. Duku et al. (2008) found that the material-specific constant a varied as a function of Dr and σ'_v, and proposed the following relationship for a for σ'_v = 1 atm (i.e., $a_{1\ atm}$):

$$a_{1\ atm} = 5.38 \cdot exp(-0.023 \cdot Dr\%) \quad (2c)$$

To compute a for different effective overburden stresses, Eq. (2c) is multiplied by following overburden correction factor:

$$K_{\sigma,\varepsilon} = \frac{a_\sigma}{a_{1\ atm}} = \left(\frac{\sigma'_v}{P_a}\right)^{-0.29} \quad (2d)$$

Duku et al. (2008) found that b and R could be treated as constants for the clean sands tested when used in conjunction with the above expression for a: b = 1.2 and R = 0.29. Furthermore, they found that mean grain size, uniformity coefficient, particle angularity, soil fabric, mineralogy, and void ratio "breadth" (i.e., void ratio minus minimum void ratio: e-e_{min}), S, and age do not significantly influence the seismic compression response of clean sands. Accordingly, the resulting simplified expression used to compute volumetric strain is:

$$\varepsilon_v = K_{\sigma,\varepsilon} \cdot a_{1\ atm} \cdot \left(\gamma_{eff} - \gamma_{tv}\right)^b \cdot C_N \quad (2e)$$

Yee et al. (2014) continued the work of Duku et al. (2008) by testing non-plastic to moderately plastic silty sands/sandy silts (i.e., PI ≤ 10), with FC ranging from 0 to 60%. In contrast to clean sands, Yee et al. (2014) found that FC and S influence the volumetric strain behavior of the silty sands/sandy silts tested. For consistency, Yee et al. (2014) used the same functional form of the

equations proposed by Duku et al. (2008), but proposed the following "correction" factors for FC and *S*.

Fines content (FC):

$$K_{FC} = \frac{a_{FC}}{a_{FC=0}} = \begin{cases} 1 & \text{if } 0 \le FC \le 10\% \\ e^{-0.042 \cdot (FC-10)} & \text{if } 10\% < FC < \sim 35\% \\ 0.35 & \text{if } FC \ge \sim 35\% \end{cases} \quad (3a)$$

Saturation (*S*):

$$K_S = \frac{a_S}{a_{S=0}} = \begin{cases} -0.017 \cdot S + 1 & \text{if } S < 30\% \\ 0.5 & \text{if } 30\% \le S < 50\% \\ 0.05 \cdot S - 2 & \text{if } 50\% \le S < 60\% \\ 1 & \text{if } S \ge 60\% \end{cases} \quad (3b)$$

Accordingly, the resulting simplified expression to compute volumetric strain is:

$$\varepsilon_v = K_{FC} \cdot K_S \cdot K_{\sigma,\varepsilon} \cdot a_{1\ atm\ \&\ FC=0\ \&\ S=0} \cdot \left(\gamma_{eff} - \gamma_{tv}\right)^b \cdot C_N \quad (3c)$$

Although Yee et al. (2014) found that it was reasonable to assume that *b* can be treated as a constant and having the same values as determined by Duku et al. (2008) for clean sands (i.e., $b = 1.2$), they found that *R* cannot be treated as a constant. Rather, Yee et al. (2014) found that *R* varied as a function of the imposed shear strain:

$$R = -0.026 \cdot \ln\left(\gamma_{eff} - \gamma_{tv}\right) + 0.26 \quad (3d)$$

2.3.2 Non-Simplified Procedures

As mentioned in the Introduction, only a few non-simplified procedures have been proposed for evaluating seismic compression (e.g., Martin et al. 1975; Finn and Byrne 1976; Byrne 1991; Nasim and Wartman 2006; Lasley et al. 2016). Most significantly, Byrne (1991) proposed the following variant of the Martin et al. (1975) non-simplified model to estimate volumetric strains in dry sands:

$$\varepsilon_v = \sum_i \left(\Delta\varepsilon_{v,1/2}\right)_i \quad (4a)$$

where ε_v = accumulated volumetric strain in percent at the end of loading; and $(\Delta\varepsilon_{v,1/2})_i$ = increment in volumetric strain in percent at the end of the i^{th} half-shear strain cycle of loading

having an amplitude γ_i. For earthquake loading, γ_i is typically taken as the peak shear strain between two zero crossings in the shear strain time history (e.g., Green and Terri 2005). $(\Delta\varepsilon_{v,1/2})_i$ is computed as:

$$\left(\Delta\varepsilon_{v,1/2}\right)_i = 0.5 \cdot (\gamma_i - \gamma_{tv}) \cdot C_1 \cdot exp\left[-C_2 \frac{\varepsilon_{vi}}{(\gamma_i - \gamma_{tv})}\right] \quad (4b)$$

where C_1 and C_2 are material-specific parameters; and ε_{vi} is the volumetric strain in percent at the beginning of the i^{th} load increment. Based on the analysis of the laboratory data for Crystal Silica Sand No. 2 from Silver and Seed (1971) and Seed and Silver (1972) (i.e., the same data used by Tokimatsu and Seed 1987), Byrne (1991) provided expressions to estimate C_1 and C_2:

$$C_1 = 7{,}600 \cdot Dr\%^{-2.5} \quad (4c)$$

$$C_2 = \frac{0.4}{C_1} \quad (4d)$$

Although neither Martin et al. (1975) nor Byrne (1991) make reference to fatigue theories, their models are inherently load dependent, interaction macro-level fatigue models in which ε_v is used as the damage metric (e.g., Kaechele 1963). This means that the nature of the accumulation of volumetric strain is a function of the amplitude of the load and is influenced by previous loading (i.e., sequencing of the pulses in a loading history influences the resulting volumetric strain) (Green and Lee 2006; Lasley et al. 2016a, 2017). The basis for this type of model comes directly from the observed volumetric strain behavior in laboratory tests, with this behavior largely ignored by the procedures used to develop many of the existing $n_{eq\tau}$ and $n_{eq\gamma}$ relationships (more details on this are provided in Green and Terri 2005, and Green and Lee 2006).

Lasley et al. (2016a) proposed a variant of the macro-level fatigue model by Richart-Newmark (1948) (i.e., the R-N model) for evaluating seismic compression. The R-N model has the general form:

$$D = H^r \quad (5a)$$

where: D is the accumulated "damage" (e.g., ε_v); H is the cycle ratio (i.e., the ratio of number of applied cycles having a given amplitude to the number of cycles of that amplitude required to cause "failure" in the material: $H = n/N$); and r is a material-specific parameter that varies as a function of the amplitude of loading (e.g., γ). For evaluating seismic compression due to earthquake loading, Eq. (5a) expands to:

$$\varepsilon_{v_i} = \left[\left(\varepsilon_{v_{i-1}}\right)^{1/r_i} + \left(\frac{n_i}{N_i}\right)\right]^{r_i} \quad (5b)$$

where ε_{vi} is the volumetric strain at the end of the i^{th} load increment. To introduce the interaction behavior to the model, Lasley et al. (2016a) made r a function of H (i.e., the nature of the

accumulation of volumetric strain is influence by previous loading). Unfortunately, this makes the model somewhat difficult to implement (e.g., Yee and Stewart 2018), which is a significant impediment to its use. As a result, the Byrne (1991) model is used as the basis for advancing non-simplified seismic compression procedures herein because it is easier to implement than the modified R-N model proposed by Lasley et al. (2016a).

2.4 Expanded Byrne (1991) Model

2.4.1 Simplified Form of the Byrne Model

As detailed in the Appendix, the Byrne model can be written in the alternative form:

$$\varepsilon_{v_i} = -ln(\prod_i t_i) \cdot \frac{(\gamma_i - \gamma_{tv})}{C_2} \tag{6a}$$

where:

$$t_i = \begin{cases} e^{-0.5 \cdot C_1 \cdot C_2} & if\ i = 1 \\ (t_{i-1})^{t_{i-1}} & if\ i > 1 \end{cases} \tag{6b}$$

and ε_{vi} is the volumetric strain in percent at the end of the i^{th} load increment having amplitude γ_i (γ_i and γ_{tv} are both in percent). If the seismic demand is expressed in terms of γ_{eff} and $n_{eq\gamma}$, Eq. (6a) can be written in simplified form:

$$\varepsilon_v = -ln\left(\prod_{i=1}^{2 \cdot n_{eq\gamma}} t_i\right) \cdot \frac{(\gamma_{eff} - \gamma_{tv})}{C_2} \tag{6c}$$

Figure 2a shows the computed values of $\varepsilon_{v,15}$ as a function of γ_{eff} using Eq. (6c) for two different values of γ_{tv}, plotted in the same form as the relationship proposed by Tokimatsu and Seed (1987) (Figure 1a). Recall that both the Tokimatsu and Seed (1987) and Byrne (1991) models were calibrated using the same clean sand data from Silver and Seed (1971) and Seed and Silver (1972), with this data also shown in Figure 2a. As may be observed from Figure 2a, Eq. (6c) predicts $\varepsilon_{v,15}$ values for a given Dr that deviate from a straight line on log-log scale as the γ_{eff} approaches the γ_{tv}, when $\gamma_{tv} > 0$. This deviation is supported to some extent by the laboratory test data shown.

Eq. (6c) can be used to compute C_N as a function of $n_{eq\gamma}$ by computing the ratio of ε_v for a given value of $n_{eq\gamma}$ and for $n_{eq\gamma} = 15$ for the same γ_{eff}:

$$C_N = \frac{\varepsilon_{v_i}}{\varepsilon_{v,15}} = \frac{ln(\prod_i t_i)}{ln\left(\prod_{j=1}^{30} t_j\right)} \tag{7}$$

Recall that i is the number of half cycles, so $i = 30$ corresponds to $n_{eq\gamma} = 15$ cycles.

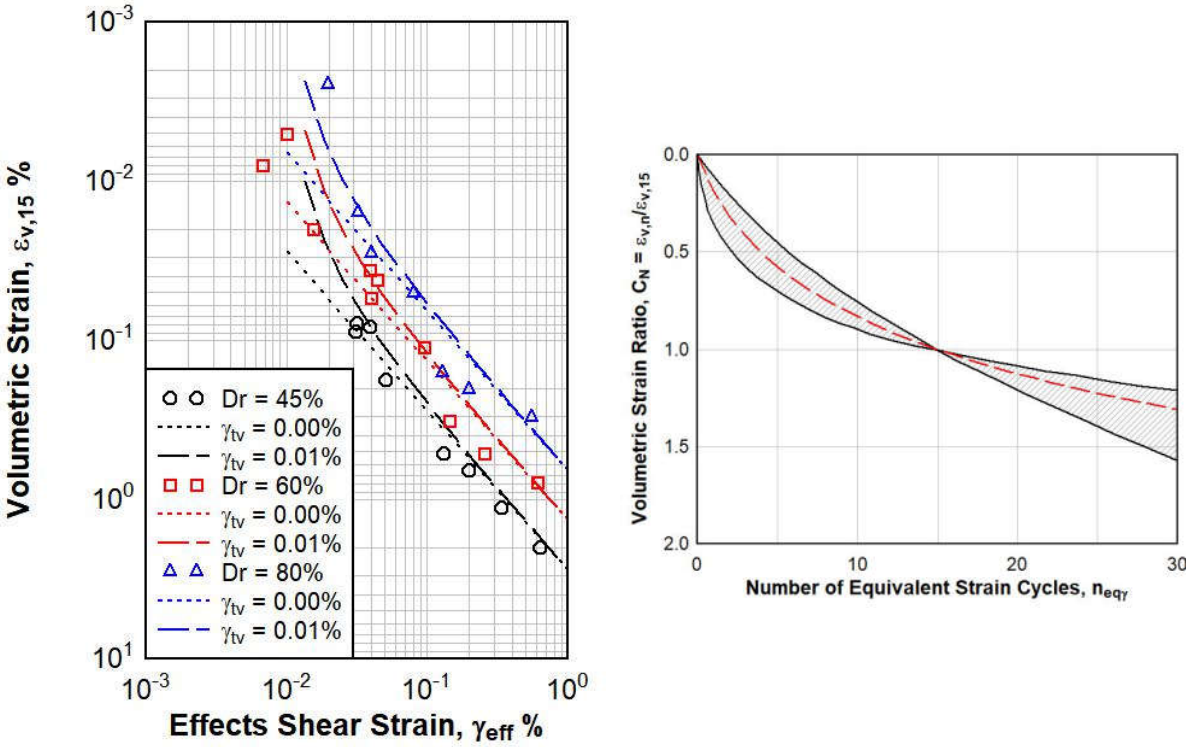

(a) (b)

Figure 2: Predictions made by the simplified form of the Byrne model, Equations (6) and (7): (a) Relationship between $\varepsilon_{v,15}$ vs. γ_{eff} for γ_{tv} = 0 and 0.01%, along with laboratory data from Silver and Seed (1971) and Seed and Silver (1972); and (b) relationship between C_N and $n_{eq\gamma}$.

As shown in Figure 2b, the predicted values of C_N fall well within the range of values from the Silver and Seed (1971) and Seed and Silver (1972) data.

2.4.2 Calibration of the Expanded Byrne Model

Comparison of Equations (2e) and (6c) implies that:

$$\frac{-ln\left(\prod_{i=1}^{2\cdot n_{eq\gamma}} t_i\right)}{C_2} = K_{\sigma,\varepsilon} \cdot a_{1\,atm} \cdot C_N$$

and

$$b = 1$$

This forms the basis for expanding and calibrating the Byrne model to evaluate seismic compression in soils other than just clean sands. Specifically, to account for soils that exhibit seismic compression behavior for $b \neq 1$, the simplified form of the Byrne model can be expanded to:

$$\varepsilon_v = -ln\left(\prod_{i=1}^{2 \cdot n_{eq\gamma}} t_i\right) \cdot \frac{(\gamma_{eff} - \gamma_{tv})^{C_3}}{C_2} \quad (8a)$$

or

$$\left(\Delta\varepsilon_{v,1/2}\right)_i = 0.5 \cdot (\gamma_i - \gamma_{tv})^{C_3} \cdot C_1 \cdot exp\left[-C_2 \frac{\varepsilon_{vi}}{(\gamma_i - \gamma_{tv})^{C_3}}\right] \quad (8b)$$

for the non-simplified form. Eq. (8b) is actually proposed in the recent and independent study by Chen et al. (2019) based on the analysis of excess pore water generation in undrained cyclic triaxial test samples, giving further credence to this expanded form.

Calibrating Eq. (8a) using the data and model from Duku et al. (2008) for clean sands:

$$C_1 = \frac{1}{2.8001} \cdot K_{\sigma,\varepsilon} \cdot a_{1\ atm} \quad (9a)$$

$$C_2 = \frac{1}{C_1} \quad (9b)$$

$$C_3 = 1.2 \quad (9b)$$

and using the data and model from Yee et al. (2014) for non-plastic to moderately plastic silty sands/sandy silts (i.e., PI ≤ 10), with FC ranging from 0 to 60%:

$$C_1 = \frac{1}{F_P(\gamma)} \cdot K_{FC} \cdot K_S \cdot K_{\sigma,\varepsilon} \cdot a_{1\ atm\ \&\ FC=0\ \&\ S=0} \quad (10a)$$

$$F_P(\gamma) = 2.149 \cdot \gamma^{-0.2343} + 4.337 \cdot e^{-66.56 \cdot \gamma} \quad (10b)$$

$$C_2 = \frac{P(\gamma)}{C_1} \quad (10c)$$

$$P(\gamma) = e^{0.405} \cdot (\gamma - \gamma_{tv})^{0.3291} \quad (10d)$$

$$C_3 = 1.2 \quad (10e)$$

where γ and γ_{tv} are in percent. Details about how the calibration was performed are provided in the Appendix. The expressions for C_1, C_2, and C_3 given by Equations (9) and (10) can be used in conjunction with the simplified and non-simplified forms of the expanded Byrne model, Equations (8a) and (8b), respectively. Note that when used in conjunction with the simplified form, γ in Equations (10a,b,c,d) is γ_{eff}, and when used in conjunction with the non-simplified γ is γ_i. In the following section, both forms of the expanded Byrne model are used to analyze a field case history from the 2007, moment magnitude (M_w) 6.6 Niigata-ken Chuetsu-oki, Japan, earthquake.

2.5 Case History Analysis

2.5.1 Background

The main shock of the M_w6.6 Niigata-ken Chuetsu-oki Japan earthquake occurred on 16 July 2007. The event affected an ~100-km-wide area along the coastal regions of southwestern Niigata prefecture and triggered ground failures as far as the Unouma Hills, located in central Niigata approximately 50 km from the shore (Kayen et al. 2009). Of specific interest to this study is the seismic compression that occurred during this event at the Kashiwazaki-Kariwa Nuclear Power Plant (KKNPP) site (Yee et al. 2011). What makes this case history of particular value is that the motions at the site were recorded by a free-field downhole array (Service Hall Array, SHA) and the magnitude of the seismic compression was accurately determined from the settlement of soil around a vertical pipe housing one of the array seismographs. The geometric mean of the peak accelerations at bedrock and the ground surface were 0.55g and 0.4g, respectively, indicating nonlinear site response. The seismic compression at the site was ~10-20 cm.

Yee et al. (2011) performed a detailed site investigation and determined that the profile at the strong motion array consists of ~70 m of medium-dense sands overlying clayey bedrock and that the ground water table (gwt) is at a depth of ~45 m. Suspension logging and Standard Penetration Tests (SPT) with energy measurements were performed at the site, with the former providing small-strain shear and compression wave velocities (i.e., Vs and Vp, respectively). Additionally, laboratory tests were performed on disturbed and undisturbed samples to classify the soil, to determine index properties and shear strength of the soil, and to develop modulus reduction and damping (MRD) curves. The geologic log and instrument locations for the SHA site are shown in Figure 3. Also, shown in this figure are the results SPT and suspension logging geophysical testing and some of their interpretation.

2.5.2 Site Response Analysis

One-dimensional equivalent linear (EQL) site response analyses were performed for the site using the software Strata (Kottke and Rathje 2009) following the modeling details in Yee et al. (2011, 2013). The motions recorded by the array were obtained from Professor Jonathan Stewart, UCLA; the motions had been processed following the procedures used to process the motions in the PEER Ground Motion Database (PEER 2019). The motions were oriented in the EW and NS directions, and those corresponding to a depth of 99.4 m were specified as "within" input motions in the EQL analyses. The motions are shown in Figure 4.

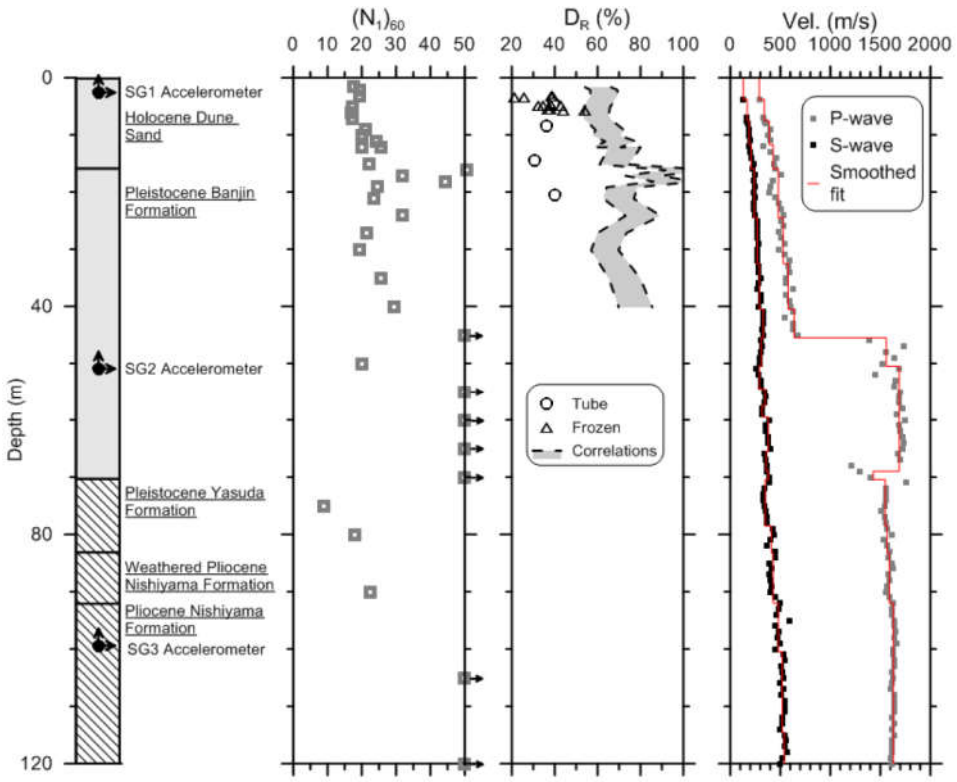

Figure 3: Geologic log for the SHA site including instrument locations and data SPT and suspension logging geophysical testing (Yee et al. 2011).

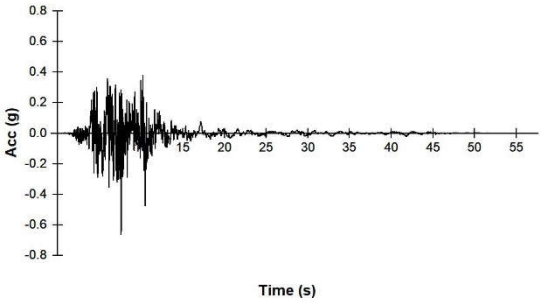

(a)

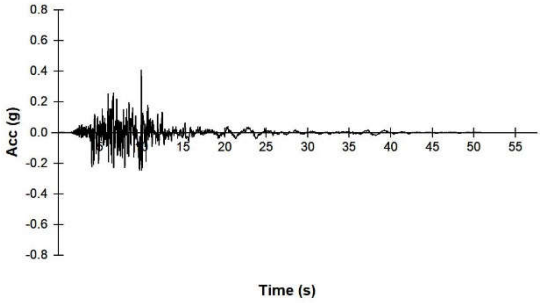

(b)

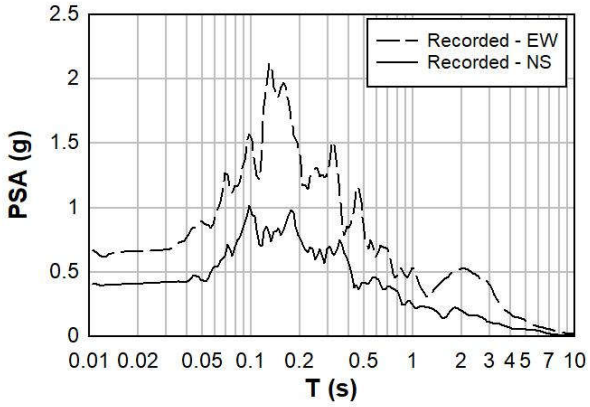

(c)

Figure 4: Ground motions at a depth of 99.4 m: (a) EW acceleration time history; (b) NS acceleration time history; and (c) corresponding pseudo spectral

accelerations.

The Vs profile used in the analyses is shown in Figure 5, and the total unit weights (γ_t) of the soil are listed in Table 1. The Menq (2003) MRD curves were used to model the sandy soil above the gwt, with the Yee et al. (2013) strength-adjustment applied and a minimum damping of 5% used. To account for the influence of effective confining stress, the reference strain (γ_r) used in the Menq (2003) modulus reduction curves (i.e., curves of $(G/G_{max})\gamma_{eff}$ vs. γ_{eff}) were adjusted using:

$$\gamma_r = \gamma_{r,1} \cdot \left(\frac{\sigma'_o}{P_a}\right)^n \tag{11}$$

where σ'_o is the mean effective confining stress; Pa is atmospheric pressure in the same units as σ'_o; $\gamma_{r,1}$ is the reference strain for σ'_o = 1 atm; and *n* is an empirical soil-specific factor. Based on the MRD test data for sandy soils above the gwt from the site, $\gamma_{r,1}$ = 0.0904 and *n* = 0.4345. No samples from below the gwt from the site were tested, and it was assumed that the $\gamma_{r,1}$ and *n* values proposed by Menq (2003) applied for sandy soils below the gwt: $\gamma_{r,1}$ = 0.0684 and *n* = 0.4345. The Darendeli (2001) MRD curves were used for the relatively plastic soils and rock materials below 70 m.

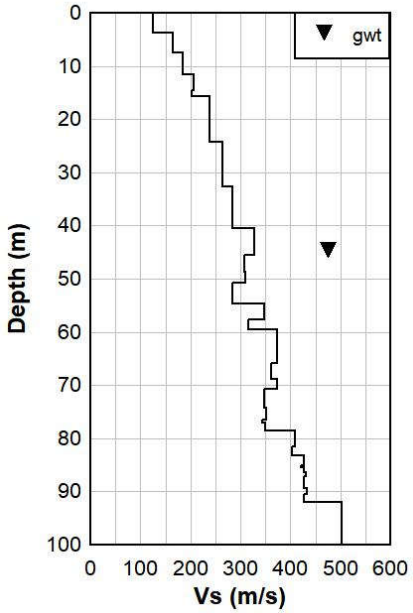

Figure 5: Small strain shear wave velocity (Vs) profile used in the Strata analyses.

Table 1: Assumed soil types and unit weights used in analysis (Motamed et al. 2016)

Depth range (m)	Soil type	Total unit weight, γ_t (kN/m^3)
0-4	Sand	16
4-45	Sand	17.75
45-70	Sand	20.8

70-99.4	Clay	20.8

To validate the EQL model, computed and recorded motions were compared at depths of 2.4 m and 50.8 m. As shown in Figure 6, the PGAs for the recorded and computed motions are in good agreement, as are the response spectra. Accordingly, the EQL model was used to compute the shear strain time histories at the center of each of the model layers above 45 m (i.e., above the gwt). As discussed next, these time histories were used to compute the ε_v in each layer and the overall settlement at the site due to seismic compression.

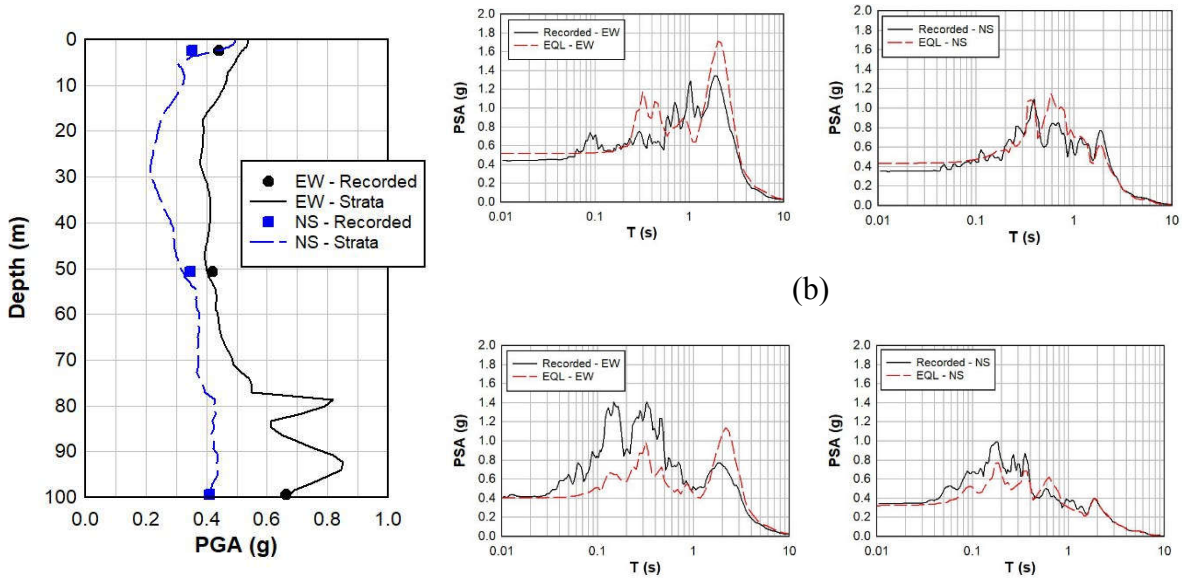

Figure 6: Results used to validate EQL model used to compute shear strain time histories at varying depths in the SHA profile: (a) Comparison of computed and recorded PGAs; (b) comparison of response spectra for computed and recorded motions at a depth of 2.4 m (NS-left; EW-right); and (c) comparison of response spectra for computed and recorded motions at a depth of 50.8 m (EW-left; NS-right).

2.5.3 Seismic Compression

Yee et al. (2011) performed a series of drained cyclic simple shear tests on samples from the KKNPP site and developed soil-specific calibration parameters for the Duku et al. (2008) simplified model (Eq. 2) for Dr ≈ 35% and 60%. These calibration parameters are listed in Table 2. Using these, the calibration parameters for the expanded Byrne model were computed:

$$C_1 = K_{\sigma,\varepsilon} \cdot 1.28 \cdot e^{-0.019 \cdot Dr\%} \quad (12a)$$

$$C_2 = \frac{0.7864}{C_1} \quad (12b)$$

$$C_3 = 1.2 \quad (12c)$$

Figure 7 shows a comparison of the $\varepsilon_{v,15}$ vs. γ_{eff} and C_N vs. $n_{eq\gamma}$ for the Duku et al. (2008) and expanded Byrne model using the KKNPP soil-specific calibration parameters. As may be observed from these plots, the model predictions are in very good agreement.

Table 2: KKNPP soil-specific calibration parameters for the Duku et al. (2008) model.

	Dr ≈ 35%	Dr ≈ 60%
$a_{1\ atm}$	2.15	1.33
b	1.2	1.2
R	0.31	0.31
γ_{tv}	0.03%	0.03%

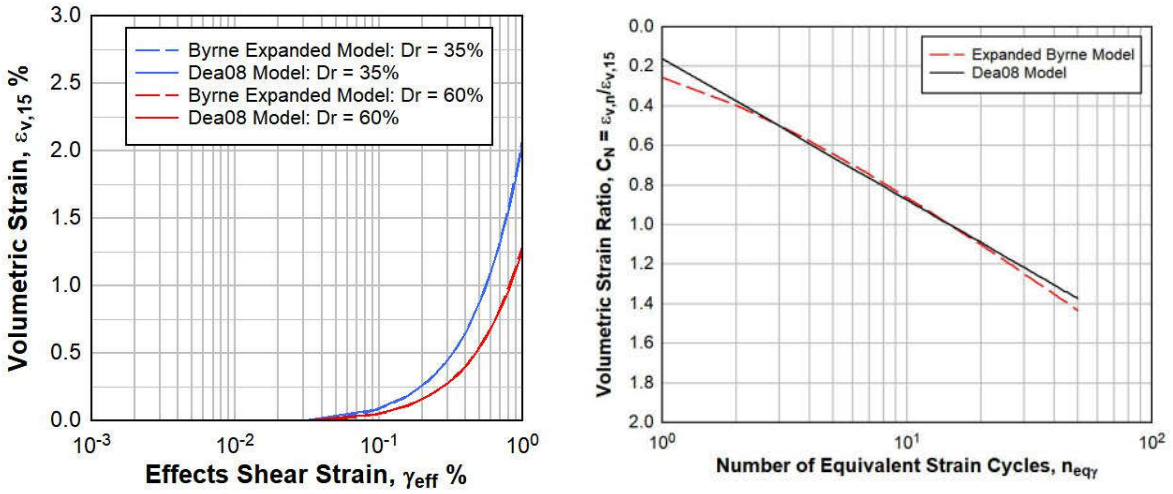

(a) (b)pe

Figure 7: Comparison of (a) $\varepsilon_{v,15}$ vs. γ_{eff} and (b) C_N vs. $n_{eq\gamma}$ for the Duku et al. (2008) and expanded Byrne model using the KKNPP soil-specific calibration parameters.

Dr for the soil were estimated using the relationship:

$$Dr\% = 100 \cdot \sqrt{\frac{N_{1,60}}{C_d}} \tag{13}$$

where $N_{1,60}$ is the corrected SPT blow count, and C_d is a soil-specific parameter. Per Skempton (1986), C_d was assumed to be 55 (natural deposit of fine sand).

The non-simplified expanded Byrne model (Eq. 8b) calibrated using Eq. (12) was used in conjunction with the shear strain time histories computed at the center of each of the Strata model layers above the gwt. The total settlement at the ground surface (S_T) at the site was then computed from the resulting ε_v values for each layer:

$$S_T = \sum_j \varepsilon_{v_j} \cdot \Delta z_j \tag{14}$$

where ε_{vj} is the volumetric strain in the j^{th} layer; and Δz_j is the thickness of the j^{th} layer. The EW and NS motions were computed to ~3.5 cm and ~1.2 cm of seismic compression, respectively, resulting in a geometric mean settlement of ~2 cm. Based on a series of numerical analyses with soil elements subjected to multidirectional motions, wherein the soil response was modeled using a reduced-order bounding surface hypoplasticity model (Li et al. 1992), Lasley and Green (2012) proposed the values tabulated in Table 3 to relate seismic compression in soil subjected to geometric mean motions to that resulting from the soil being subjected to two horizontal components of motions simultaneously (also see Nie et al. 2017). Based on the Dr shown in Figure 3 and computed using Eq. (13), a conversion factor (C_{2D}) of 1.8 is appropriate for this site/earthquake. Also, based on the work of Pyke et al. (1975) vertical motions can increase the seismic compression between 20% and 50% as the peak vertical accelerations range from 0.15g to 0.3g. Yee et al. (2011) recommend using an effective peak vertical acceleration of 0.4g for the SHA site. Using this value for vertical acceleration increases the seismic compression by 50%, and results in a predicted seismic compression of ~5.5 cm (1.8×1.5×2 cm = 5.5 cm).

Table 3: Correction Factor, C_{2D}, for Two-Dimensional Shaking (Lasley and Green 2012).

Dr (%) ($N_{1,60}$)	Moment Magnitude, M_w		
	5-6	6-7	7-8
45 (9)	1.5	1.6	1.7
60 (17)	1.9	1.8	1.8
80 (30)	2	1.9	1.8
100 (46)	2	2.1	2.1

The simplified expanded Byrne model (Eq. 8a) calibrated using Eq. (12) was used in conjunction with the γ_{eff} values computed using Eq. (1). Eq. (1) was solved iteratively using the shear modulus reduction curves used in the Strata analyses and a_{max} = 0.4g (i.e., geometric mean of the recorded peak accelerations at ground surface). The r_d relationship proposed by Idriss (1999) was used. Although Lasley et al. (2016b) shows that this relationship generally predicts too rigid of profile response for liquefaction triggering analyses, the profiles for seismic compression analyses tend to be stiffer than sites evaluated for liquefaction due to deeper gwt (or higher effective confining stresses). As a result, it is recommended that the Idriss (1999) r_d relationship be used to compute γ_{eff} in seismic compression analyses.

Figure 8 is a plot of the γ_{eff} computed using Eq. (1) and computed from the shear strain time histories from the EQL analyses. For the latter values, γ_{eff} was computed as 0.65 times the geometric mean of the peak shear strains in each layer resulting from the Strata analyses using the EW and NS motions. As may be observed from Figure 8, γ_{eff} computed using Eq. (1) have a similar trend with depth as those from the Strata analyses, but are slightly larger in magnitude for most depths.

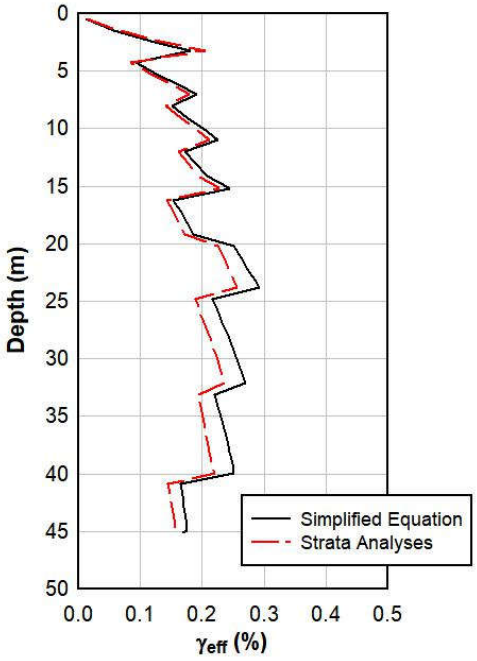

Figure 8: Comparison of γ_{eff} computed using the Eq. (1) and from the Strata analyses.

The relationship proposed by Lee and Green (2017) was used to compute $n_{eq\gamma}$:

$$ln(n_{eq\gamma}) = \exp(b_1 \cdot z) + b_2 \cdot {R_{rup}}^{b_3} + b_4 \cdot M_w + b_5 \quad (15)$$

where z is depth below the ground surface in m; R_{rup} is the closest distance to the fault rupture plane (km); and b_1-b_5 are regression coefficients. Yee et al. (2011) give R_{rup} = 16 km and values of b_1-b_5 are listed in Table 4 for stable continental and active tectonic regimes (e.g., Central-Eastern US, CEUS, and Western US, WUS, respectively). This relationship is preferred over others because it was specifically developed for computing the $n_{eq\gamma}$ for seismic compression analyses. Its use is in contrast to the common practice of using $n_{eq\tau}$ relationships developed for liquefaction triggering analyses in seismic compression analyses, not recognizing the potential differences between $n_{eq\gamma}$ and $n_{eq\tau}$ (see details in Green and Terri 2005). Figure 9 shows a plot of the computed $n_{eq\gamma}$ vs. depth.

Table 4: Regression coefficients and standard deviations of inter-event, intra-event, and total error (Lee and Green 2017).

CEUS							
b_1	b_2	b_3	b_4	b_5	τ_{ln}	σ_{ln}	σ_{ln_total}
-0.020	0.80	0.22	0.19	-1.30	0.26	0.47	0.54
WUS							
b_1	b_2	b_3	b_4	b_5	τ_{ln}	σ_{ln}	σ_{ln_total}

-0.0099	0.67	0.21	0.28	-1.79	0.24	0.41	0.48

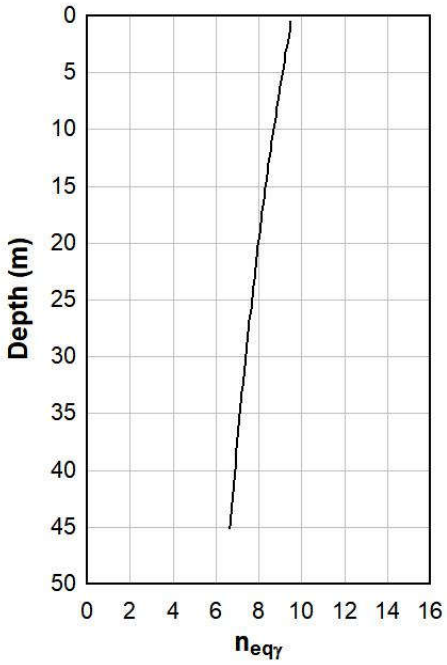

Figure 9: $n_{eq\gamma}$ as a function of depth computed using the relationship by Lee and Green (2017).

The resulting seismic compression using the expanded simplified Byrne model is ~4 cm. However, this value only reflects the seismic compression resulting from the profile being subjected to the geometric mean of the two horizontal components of motion (i.e., both the a_{max} and $n_{eq\gamma}$ were based on geometric means of the horizontal components of motion). Accounting for multidirectional shaking, the resulting settlement due to seismic compression using the expanded simplified Byrne model is ~10.4 cm (1.8×1.5×4 cm = 10.4 cm).

2.6 Discussion and Conclusions

Together the simplified and non-simplified forms of the expanded Byrne model provide a versatile approach for evaluating seismic compression that is scalable based on available data and the importance of the project. Both forms of the model use the same calibration parameters, which have been developed herein for clean sands and non-plastic to moderately plastic (PI ≤ 10) silty sands/sandy silts using the extensive laboratory data performed by researchers at the University of California at Los Angeles. The non-simplified form is relatively easy to implement and thus, overcomes the complexity issues with implementing other non-simplified models (e.g., Lasley et al. 2016a).

Both the simplified and non-simplified expanded Byrne models were used to evaluate seismic compression at the KKNPP SHA site during the main shock of the 2007, M_w6.6 Niigata-ken

Chuetsu-oki, Japan, earthquake. The non-simplified model was used in conjunction with shear strain time histories computed at varying depths in the profile using EQL site response analyses. The geometric mean settlement at the ground surface due to horizontal shaking was ~2 cm, but this value increases to ~5.5 cm when the influence of multidirectional shaking is considered. The simplified model predicts ~4 cm of settlement at the ground surface when the horizontal geometric mean motions are considered. However, this value increases to ~10.4 cm when all three dimensions of shaking are considered.

The predicted settlement using the non-simplified, expanded Byrne model is about half of the lower end of the range of observed settlements (10-20 cm), while that predicted settlement using the simplified variant is about equal to lower end of the observed range. Given that the site was very well characterized, the site response model was validated and the motions used in modeling were those that were recorded at the site, and the seismic compression model was calibrated using soil from the site, it is difficult to identify why the predicted surface settlement is on the low end. One potential reason is the Dr values estimated using SPT blow count via Equation (13), with the resulting values being ~60% for most depths. This value is about double that determined from samples (triple-barrel pitcher samples and frozen samples) which were ~30%-40%, as shown in Figure 3. Assuming the Dr = 35% for all depths results in predicted settlements of 10 cm and 19 cm using the non-simplified and simplified variants of the expanded Byrne model, respectively. These predicted values are good accord with field observations, giving credence to the Dr estimation being the reason for the initial under-predictions.

The larger computed settlements using the simplified vs. non-simplified variant relates to the $n_{eq\gamma}$ estimated using the Lee and Green (2017) relationship, given that the γ_{eff} values for the simplified procedure are approximately equal to those from the site response analyses (Figure 8). An argument can be made that it is appropriate for simplified models to be somewhat conservative in their predictions, providing the impetus for more detailed analyses to be performed (i.e., implementation of non-simplified procedures and the inherent more detailed site and seismic characterizations). However, it is doubtful that the simplified variant of the expanded Byrne model will always predict larger settlements than the non-simplified variant because there are not any intentional conservative biases inherent to the simplified variant. Accordingly, the non-simplified procedure can be viewed as providing a more accurate estimate of the predicted seismic compression, assuming the required inputs to the analysis are accurate, not necessarily a lower predicted value of seismic compression. Accounting for the differences in the uncertainties inherent to the predictions made using simplified vs. non-simplified procedures should be introduced via the criteria used to set acceptable magnitudes of seismic compression for the procedures.

In the author's view, the greatest uncertainty in the predictions using both forms of the expanded Byrne model is accounting for the influence of vertical shaking. This is because few studies have examined this issue (i.e., the author is only aware of the study by Pyke et al. 1975), and

the resulting adjustments increase the predicted seismic compression by 20% - 50%. Also, the Tokimatsu and Seed (1987) simplified procedure for evaluating seismic compression ignores the influence of vertical motions, which is interesting given that Professor H.B. Seed was directly involved in both the Pyke et al. (1975) and the Tokimatsu and Seed (1987) studies. Accordingly, seismic compression evaluations would benefit from a more detailed analysis of the influence of vertical motions on seismic compression, as well as the development of calibration parameters for additional types of soils/states.

References

Byrne, P. (1991). "A cyclic shear-volume coupling and pore pressure model for sand." *Proc., 2nd Int. Conf. on Recent Advances in Geotechnical Earthquake Engineering and Soil Dynamics*, Missouri Univ. of Science and Technology, Rolla, MO, 47–55.

Carter, W.L., Green, R.A., Bradley, B.A., Wotherspoon, L.M., and Cubrinovski, M. (2016). "Spatial Variation of Magnitude Scaling Factors During the 2010 Darfield and 2011 Christchurch, New Zealand, Earthquakes," *Soil Dyn. Earthquake Engrg.*, 91, 175-186.

Chen, G., Zhao, D., Chen, W., and Juang, C.H. (2019). "Excess pore-water pressure generation in cyclic undrained testing." *J. Geotech. Geoenviron. Eng.*, 145(7), 04019022.

Chu, H.-H. and Vucetic, M. (1992). "Settlement of compacted clay in a cyclic direct simple shear device." *Geotech. Test. J.*, 15(4), 371–379.

Darendeli, M. (2001). "Development of a new family of normalized modulus reduction and material damping curves," *Ph.D. Dissertation*, Dept. of Civil Eng., Univ. of Texas, Austin, TX.

Duku, P.M., Stewart, J.P., Whang, D.H., and Yee, E. (2008). "Volumetric strains of clean sands subject to cyclic loads," *J. Geotech. Geoenviron. Eng.*, ASCE, 134 (8), 1073-1085.

Finn, W. D. L., and Byrne, P. M. (1976). "Estimating settlements in dry sands during earthquakes." *Can. Geotech. J.*, 13(4), 355–363.

Green, R.A. and Lee, J. (2006). "Computation of number of equivalent strain cycles: A theoretical framework." *Geomechanics II: Testing, modeling, and simulation*, P. V. Lade and T. Nakai, eds., ASCE, Reston, VA, 471–487.

Green, R. A., and Terri, G. A. (2005). "Number of equivalent cycles concept for liquefaction evaluations—Revisited." *J. Geotech. Geoenviron. Eng.*, 10.1061/(ASCE)1090-0241(2005) 131:4(477), 477–488.

Hancock, J. and Bommer, J. J. (2005). "The effective number of cycles of earthquake ground motion." *Earthquake Eng. Struct. Dyn.*, 34(6), 637–664.

Hsu, C.-C., and Vucetic, M. (2004). "Volumetric threshold shear strain for cyclic settlement." *J. Geotech. Geoenviron. Eng.*, 10.1061/(ASCE) 1090-0241(2004)130:1(58), 58–70.

Idriss, I.M. (1999). "An update to the Seed-Idriss simplified procedure for evaluating liquefaction potential." *Proc., TRB Workshop on New Approaches to Liquefaction Analysis*, U.S. Dept. of Transportation, Federal Highway Administration, Washington, DC.

Kaechele, L. (1963). *Review and analysis of cumulative-fatigue-damage theories*. Memorandum RM-3650-PR, Rand Corporation, Santa Monica, CA.

Kayen, R., Brandenberg, S.J., Collins, B.D., Dickenson, S., Ashford, S., Kawamata, Y., Tanaka, Y., Koumoto, H., Abrahamson, N., Cluff, L., Tokimatsu, K. (2009). "Geoengineering and seismological aspects of the Niigata-ken Chuetsu-oki earthquake of 16 July 2007," *Earthquake Spectra*, 25(4), 777–802.

Kottke A., and Rathje, E.M. (2009). *Technical Manual for Strata*. PEER 2008/10, Pacific Earthquake Engineering Research Center, University of California at Berkeley, Berkeley, CA.

Lasley, S. and Green, R. A. (2012). *Evaluating Seismic Compression and Post Liquefaction Settlement at Level-Ground Sites*. Center for Geotechnical Practice and Research (CGPR) Report #69, The Charles E. Via, Jr., Department of Civil and Environmental Engineering, Virginia Tech, Blacksburg, VA.

Lasley, S., Green, R.A., Chen, Q., and Rodriguez-Marek, A. (2016a). "Approach for Estimating Seismic Compression Using Site Response Analyses." *J. Geotech. Geoenviron. Eng.*, ASCE, 142(6), 04016015.

Lasley, S., Green, R.A., and Rodriguez-Marek, A. (2016b). "A New Stress Reduction Coefficient Relationship for Liquefaction Triggering Analyses." Technical Note, *J. Geotech. Geoenviron. Eng.*, ASCE, 142(11), 06016013-1.

Lasley, S., Green, R.A., and Rodriguez-Marek, A. (2017). "Number of Equivalent Stress Cycles for Liquefaction Evaluations in Active Tectonic and Stable Continental Regimes," *J. Geotech. Geoenviron. Eng.*, ASCE, 143(4), 04016116-1.

Lee, J. and Green, R.A. (2017). "Number of Equivalent Strain Cycles for Active Tectonic and Stable Continental Regions." *Proc. 19th Intern. Conf. on Soil Mechanics and Geotechnical Engineering*, Seoul, Korea, 17-22 September.

Li, X. S., Wang, Z. L., and Shen, C. K. (1992). *SUMDES: A nonlinear procedure for response analysis of horizontally-layered sites subjected to multi-directional earthquake loading*. Dept. of Civil Engineering, Univ. of California, Davis, CA.

Liu, A.H., Stewart, J.P., Abrahamson, N.A., and Moriwaki, Y. (2001). "Equivalent number of uniform stress cycles for soil liquefaction analysis," *J. Geotech. Geoenviron. Eng.*, ASCE, 127(12), 1017–1026.

Martin, G.R., Finn, W.D.L., and Seed, H.B. (1975). "Fundamentals of liquefaction under cyclic loading." *J. Geotech. Eng. Div.*, 101(GT5), 423–438.

Menq, F.Y. (2003). *Dynamic properties of sandy and gravelly soils*. *Ph.D. Dissertation*, Dept. of Civil Eng., Univ. of Texas, Austin, TX.

Motamed, R., Stanton, K., Almufti, I., Ellison, K., and Willford, M. (2016). "Improved approach for modeling nonlinear site response of highly strained soils: Case study of Service Hall Array in Japan." *Earthquake Spectra*, 32(2), 1055-1074.

Nasim, A.S. and Wartman, J. (2006). "Seismic compression analysis using a soil liquefaction constitutive model." *FLAC and Numerical Modeling in Geomechanics 2006*: Proc. 4th Int. FLAC Symp., Itasca Consulting Group, Minneapolis.

Nie, C.-X., Chen, Q.-S., Gao, G.-Y., and Yang, J. (2017). "Determination of seismic compression of sand subjected to two horizontal components of earthquake ground motions." *Soil Dyn. Earthquake Engrg.*, 92, 330-333.

PEER (2019). PEER Ground Motion Database: https://ngawest2.berkeley.edu/site (last accessed 22 August 2019).

Pyke, R., Seed, H.B., Chan, C.K. (1975). "Settlement of sands under multidirectional shaking." *J. Geotech. Engrg.*, ASCE, 101 (4), 379-398.

Sawada, S., Tsukamoto, Y., and Ishihara, K. (2006). "Residual deformation characteristics of partially saturated sandy soils subjected to seismic excitation." *Soil Dyn. Earthquake Engrg.*, 26(2–4), 175–182.

Seed, H.B. and Silver, M.L. (1972). "Settlement of dry sands during earthquakes." *J. Soil Mech. Found. Div.*, 98(SM4), 381–397.

Seed, H. B., Idriss, I. M., Makdisi, F., and Banerjee, N. (1975). *Representation of irregular stress time histories by equivalent uniform stress series in liquefaction analyses*. EERC 75-29, Earthquake Engineering Research Center, Univ. of California, Berkeley, CA.

Silver, M.L. and Seed, H.B. (1971). "Volume changes in sands during cyclic loading." *J. Soil Mech. Found. Div.*, 97(SM9), 1171–1182.

Siddharthan, R.V., and El-Gamal, M. (1996). "Earthquake induced ground settlements of bridge abutment fills." *Analysis and Design of Retaining Structures*, ASCE, Reston, VA, 100–123.

Skempton, A.W. (1986). “Standard penetration test procedures and the effects in sands of overburden pressure, relative density, particle size, aging, and overconsolidation.” *Geotechnique*, 36(3), 425-447.

Slosson, J. E. (1975). “Chapter 19: Effects of the earthquake on residential areas.” Bulletin 196, California Division of Mines and Geology, Sacramento, CA.

Stafford, P.J. and Bommer, J.J. (2009). “Empirical equations for prediction of the equivalent number of cycles of earthquake ground motion.” *Soil Dyn. Earthquake Engrg.*, 29(11–12), 1425–1436.

Stewart J.P., Smith P.M., Whang D.H., and Bray J.D. (2004a). “Seismic compression of two compacted earth fills shaken by the 1994 Northridge earthquake.” *J. Geotech. Geoenviron. Eng.*, ASCE, 130(5), 461-476.

Stewart, J. P., Whang, D. H., Moyneur, M., and Duku, P. (2004b). "Seismic compression of as-compacted fill soils with variable levels of fines content and fines plasticity." Consortium of Universities for Research in Earthquake Engineering, Richmond, CA.

Tokimatsu, K. and Seed, H.B. (1987). “Evaluation of settlements in sand due to earthquake shaking.” *J. of Geotech. Engrg.*, ASCE, 113(8), 861-878.

Whang, D. (2001). *Seismic compression of compacted fills*. Ph.D. thesis, Civil and Environmental Engineering Dept., Univ. of California at Los Angeles, Los Angeles, CA.

Whang, D.H., Stewart, J.P., and Bray, J.D. (2004). “Effect of compaction conditions on the seismic compression of compacted fill soils.” *Geotech. Test. J.*, 27(4), 371–379.

Yee, E. and Stewart, J.P. (2018). “A comparison of alternative seismic compression procedures.” *Geotechnical Earthquake Engineering and Soil Dynamics V: Seismic Hazard Analysis, Earthquake Ground Motions, and Regional-Scale Assessment*, GSP 291, ASCE, Reston, VA.

Yee, E. (2011). *Investigation of nonlinear site response and seismic compression from case history analysis and laboratory testing*. Ph.D. thesis, Civil and Environmental Engineering Dept., Univ. of California at Los Angeles, Los Angeles, CA.

Yee, E., Stewart, J. P., and Tokimatsu, K. (2011). *Nonlinear site response and seismic compression at vertical array strongly shaken by 2007 Niigata-ken Chuetsu-oki earthquake*. Rep. No. 2011/107, Pacific Earthquake Engineering Research Center, Univ. of California, Berkeley, CA.

Yee, E., Stewart, J. P., and Tokimatsu, K. (2013). “Elastic and large-strain nonlinear seismic site response from analysis of vertical array recordings.” *J. Geotech. Geoenviron. Eng.*, 10.1061/(ASCE)GT.1943-5606 .0000900, 1789–1801.

Yee, E., Duku, P. M., and Stewart, J. P. (2014). “Cyclic volumetric strain behavior of sands with fines of low plasticity.” *J. Geotech. Geoenviron. Eng.*, 10.1061/(ASCE)GT.1943-5606.0001041, 04013042.

Chapter 3: Thesis conclusion

3.1 Summary

Together the simplified and non-simplified forms of the expanded Byrne model provide a versatile approach for evaluating seismic compression that is scalable based on available data and the importance of the project. Both forms of the model use the same calibration parameters, which have been developed herein for clean sands and non-plastic to moderately plastic (PI $\leq$ 10) silty sands/sandy silts using the extensive laboratory data performed by researchers at the University of California at Los Angeles. The non-simplified form is relatively easy to implement and thus, overcomes the complexity issues with implementing other non-simplified models (e.g., Lasley et al. 2016a).

Both the simplified and non-simplified expanded Byrne models were used to evaluate seismic compression at the Kashiwazaki-Kariwa Nuclear Power Plant (KKNPP) Service Hall Array (SHA) site during the main shock of the 2007, M_w6.6 Niigata-ken Chuetsu-oki, Japan, earthquake. The non-simplified model was used in conjunction with shear strain time histories computed at varying depths in the profile using EQL site response analyses. The geometric mean settlement at the ground surface due to horizontal shaking was ~2 cm, but this value increases to ~5.5 cm when the influence of multidirectional shaking is considered. The simplified model predicts ~4 cm of settlement at the ground surface when the horizontal geometric mean motions are considered. However, this value increases to ~10.4 cm when all three dimensions of shaking are considered. The predicted settlement using the non-simplified variant of the expanded Byrne model is lower than that observed in the field, and the settlement predicted using the simplified variant is on the lower end of the range observed in the field. One possible reason for this might be the relative densities used in the analyses that were estimated using the SPT N-values. When Dr values estimated based on undisturbed samples were used, the predicted settlement using both variants of the expanded Byrne model compared well with the observed settlement at the site of 10-20 cm.

3.2 Key findings

Through the investigation of the Byrne (1991) model expansion and calibration of this thesis, the key findings were summarized below:

- The Byrne (1991) model was transformed to allow it to be implemented in "simplified" and "non-simplified" manners. The transformed equations disclosed

various inherent relations among variable and parameters within the Byrne (1991) model and allowed parameter-specified coefficient regressions.

- A third coefficient C_3 was introduced in the Byrne model expressions, which greatly improved its data regression flexibility.

- Three systematic model coefficient calibration procedures were developed (see Appendix B) with re-usable MATLAB codes (see Appendix D), which provided instructions and convenience for the future model calibrations.

- Two calibrated models available for clean sand and sand with fines of low plasticity were proposed based on the UCLA model coefficients regression results.

- Both the simplified and non-simplified forms of the expanded Byrne models were used to one case study, from which the uncertainty of the settlement prediction caused by vertical shaking was argued.

3.3 Recommendations for future work

In the author's view, the greatest uncertainty in the predictions using both forms of the expanded Byrne model is accounting for the influence of vertical shaking. This is because few studies have examined this issue (i.e., the author is only aware of the study by Pyke et al. 1975), and the resulting adjustments increase the predicted seismic compression by 20% - 50%. Also, the Tokimatsu and Seed (1987) simplified procedure for evaluating seismic compression ignores the influence of vertical motions, which is interesting given that Professor H.B. Seed was directly involved in both the Pyke et al. (1975) and the Tokimatsu and Seed (1987) studies. Accordingly, seismic compression evaluations would benefit from a more detailed analysis of the influence of vertical motions on seismic compression, as well as the development of calibration parameters for additional types of soils/states.

Appendix A: Byrne (1991) Model Equation Derivation

Appendix A presented the detailed derivations of the Byrne model equations as discussed in Chapter 2. In addition, analysis as well as findings for the derived equations were also discussed in this Appendix.

1. Model Equation Derivation

If the seismic demand is expressed in terms of γ_{eff}, the Byrne model can be expressed in a simplified form:

$$\left(\Delta\varepsilon_{v,1/2}\right)_{i+1} = 0.5 \cdot \left(\gamma_{eff} - \gamma_{tv}\right) \cdot C_1 \cdot exp\left[-C_2 \frac{\varepsilon_{vi}}{(\gamma_{eff}-\gamma_{tv})}\right] \quad \text{(A. 1a)}$$

$$\varepsilon_{v(i+1)} = \left(\Delta\varepsilon_{v,1/2}\right)_{i+1} + \varepsilon_{vi} \quad \text{(A. 1b)}$$

where $\left(\Delta\varepsilon_{v,1/2}\right)_i$ = increment in volumetric strain in percent at the end of the ith half-shear strain cycle; ε_{vi} is the volumetric strain in percent at the end of the ith half-shear strain cycle;

Combining Eq. (A. 1a) and Eq. (A. 1b), results were shown below:

(1) for i = 0,

$\varepsilon_{v0} = 0$

$\left(\Delta\varepsilon_{v,1/2}\right)_1 = 0.5\, C_1\left(\gamma_{eff} - \gamma_{tv}\right)$

$\varepsilon_{v1} = \left(\Delta\varepsilon_{v,1/2}\right)_1 + \varepsilon_{v0} = 0.5\, C_1\left(\gamma_{eff} - \gamma_{tv}\right)$

(2) for i = 1,

$\varepsilon_{v1} = 0.5\, C_1\left(\gamma_{eff} - \gamma_{tv}\right)$

$\left(\Delta\varepsilon_{v,1/2}\right)_2 = 0.5\, C_1\left(\gamma_{eff} - \gamma_{tv}\right)e^{-0.5\, C_1 C_2}$

$\varepsilon_{v2} = \left(\Delta\varepsilon_{v,1/2}\right)_2 + \varepsilon_{v1} = 0.5\, C_1\left(\gamma_{eff} - \gamma_{tv}\right)(1 + e^{-0.5\, C_1 C_2})$

(3) for i = 2,

$\varepsilon_{v2} = 0.5\, C_1\left(\gamma_{eff} - \gamma_{tv}\right)(1 + e^{-0.5\, C_1 C_2})$

$\left(\Delta\varepsilon_{v,1/2}\right)_3 = 0.5\, C_1\left(\gamma_{eff} - \gamma_{tv}\right)e^{-0.5\, C_1 C_2\, (1+e^{-0.5\, C_1 C_2})}$

$$\varepsilon_{v3} = \left(\Delta\varepsilon_{v,1/2}\right)_3 + \varepsilon_{v2}$$

$$= 0.5\,C_1\left(\gamma_{eff} - \gamma_{tv}\right)e^{-0.5\,C_1C_2\,(1+e^{-0.5\,C_1C_2})} + 0.5\,C_1\left(\gamma_{eff} - \gamma_{tv}\right)(1 + e^{-0.5\,C_1C_2})$$

……

Using the above gained results and calculating the volumetric strain increment ratio of any two adjacent half shear cycle, $\frac{\left(\Delta\varepsilon_{v,1/2}\right)_{i+1}}{\left(\Delta\varepsilon_{v,1/2}\right)_i}$, the results were:

$$\frac{\left(\Delta\varepsilon_{v,1/2}\right)_2}{\left(\Delta\varepsilon_{v,1/2}\right)_1} = e^{-0.5\,C_1C_2} \qquad (\mathrm{i} = 1)$$

$$\frac{\left(\Delta\varepsilon_{v,1/2}\right)_3}{\left(\Delta\varepsilon_{v,1/2}\right)_2} = e^{-0.5\,C_1C_2e^{-0.5\,C_1C_2}} \qquad (\mathrm{i} = 2)$$

$$\frac{\left(\Delta\varepsilon_{v,1/2}\right)_4}{\left(\Delta\varepsilon_{v,1/2}\right)_3} = e^{-0.5\,C_1C_2e^{-0.5\,C_1C_2e^{-0.5\,C_1C_2e^{-0.5C_1C_2}}}} \qquad (\mathrm{i} = 3)$$

……

Assuming an intermediate coefficient $\mathrm{t} = e^{-0.5\,C_1C_2}$, the volumetric strain increment ratio of any two adjacent half shear cycle ($i \geq 1$) can be written as:

$$\frac{\left(\Delta\varepsilon_{v,1/2}\right)_{i+1}}{\left(\Delta\varepsilon_{v,1/2}\right)_i} = t_i \qquad \text{(A. 2a)}$$

Where

$$t_i = \begin{cases} e^{-0.5\cdot C_1\cdot C_2} & if\ i = 1 \\ (t_{i-1})^{t_{i-1}} & if\ i > 1 \end{cases} \qquad \text{(A. 2b)}$$

The Eq. (A. 2a) can be translated to get the volumetric strain increment ratio between the i^{th} ($i \geq 2$) half shear cycle and the first half shear cycle as presented below:

$$\frac{\left(\Delta\varepsilon_{v,1/2}\right)_i}{\left(\Delta\varepsilon_{v,1/2}\right)_1} = \frac{\left(\Delta\varepsilon_{v,1/2}\right)_2}{\left(\Delta\varepsilon_{v,1/2}\right)_1} \times \frac{\left(\Delta\varepsilon_{v,1/2}\right)_3}{\left(\Delta\varepsilon_{v,1/2}\right)_2} \times \cdots\cdots \times \frac{\left(\Delta\varepsilon_{v,1/2}\right)_i}{\left(\Delta\varepsilon_{v,1/2}\right)_{i-1}} = \prod_{i-1} t_{i-1} \qquad \text{(A. 3a)}$$

Similarly, $\Delta\varepsilon_{v,j}/\Delta\varepsilon_{v,1}$ ($j \geq 2$) is:

$$\frac{\left(\Delta\varepsilon_{v,1/2}\right)_i}{\left(\Delta\varepsilon_{v,1/2}\right)_1} = \frac{\left(\Delta\varepsilon_{v,1/2}\right)_2}{\left(\Delta\varepsilon_{v,1/2}\right)_1} \times \frac{\left(\Delta\varepsilon_{v,1/2}\right)_3}{\left(\Delta\varepsilon_{v,1/2}\right)_2} \times \cdots\cdots \times \frac{\left(\Delta\varepsilon_{v,1/2}\right)_j}{\left(\Delta\varepsilon_{v,1/2}\right)_{j-1}} = \prod_{j-1} t_{j-1} \qquad \text{(A. 3b)}$$

Combining Eq. (A. 3a) and Eq. (A. 3b), the volumetric strain increment ratio of any two specific half shear cycle can be presented as follows:

$$\frac{(\Delta\varepsilon_{v,1/2})_i}{(\Delta\varepsilon_{v,1/2})_j} = \frac{\frac{(\Delta\varepsilon_{v,1/2})_i}{(\Delta\varepsilon_{v,1/2})_1}}{\frac{(\Delta\varepsilon_{v,1/2})_j}{(\Delta\varepsilon_{v,1/2})_1}} = \frac{\prod_{i-1} t_{i-1}}{\prod_{j-1} t_{j-1}} \quad \text{(A. 3c)}$$

For $i = 0$, Eq. (A. 1a) leads to:

$$(\Delta\varepsilon_{v,1/2})_1 = 0.5\, C_1(\gamma_{eff} - \gamma_{tv}) \quad \text{(A. 4a)}$$

Combining Eq. (A. 4a), Eq. (A. 1a) and Eq. (A. 3a), the volumetric increment ratio of the i^{th} half shear cycle to the first half shear cycle can be expressed as:

$$\frac{(\Delta\varepsilon_{v,1/2})_{i+1}}{(\Delta\varepsilon_{v,1/2})_1} = e^{-\frac{C_2\varepsilon_{vi}}{\gamma_{eff}-\gamma_{tv}}} = \prod_i t_i \quad \text{(A. 4b)}$$

Eq. (A. 4b) can be translated as:

$$\varepsilon_{vi} = -\ln(\prod_i t_i)\frac{(\gamma_{eff}-\gamma_{tv})}{C_2} \quad \text{(A. 4c)}$$

According to Eq. (A. 4c), the volumetric strain ratio at any specific half shear cycle end (or the normalized volumetric strain) was derived as follows:

$$\frac{\varepsilon_{vi}}{\varepsilon_{vj}} = \ln(\prod_i t_i)/\ln(\prod_j t_j) \quad \text{(A. 5a)}$$

When $j = 30$ (the number of whole equivalent shear cycle $n_{eq\gamma} = 15$), using Eq. (A. 5a), the volumetric strain ratio C_N can be expressed:

$$C_N = \frac{\varepsilon_{vi}}{\varepsilon_{v,15}} = \frac{ln(\prod_i t_i)}{ln(\prod_{j=1}^{30} t_j)} \quad \text{(A. 5b)}$$

2. Analysis and Findings from the Derived Equations

Eq. (A. 4c) can be regarded as an alternative expression of the simplified Byrne (1991) model form. In contrast to the original Byrne (1991) model, Eq. (A. 4c) reflects the effect of the half shear cycle number on the predicted seismic compression in a more straightforward way. Also, using Eq. (A. 4c) to evaluate seismic compression does not consider the volumetric strain increment accumulation, which avoids iterated calculation.

Even though Eq. (A. 4c) manifests a pure linear dependency between ε_v and γ_{eff} (under given N and model coefficients), in most of the published laboratory test data regarding ε_v vs. γ_{eff} at given N, a power-law fit match the data better than a linear fit especially for sands having fine content. Therefore, the third coefficient C_3 was introduced into Eq. (A. 4c) as an exponent of the item $(\gamma_{eff} - \gamma_{tv})$ to control the predicted curve shape and give more fit flexibility in ε_v vs. γ_{eff} regression. Note that adding C_3 did not make significant difference in the Appendix A derivation process of the Byrne (1991) model except replacing the item $(\gamma_{eff} - \gamma_{tv})$ with $(\gamma_{eff} - \gamma_{tv})^{C_3}$. After adding C_3, Eq. (A. 4c) can be updated as shown below:

$$\varepsilon_{vi} = -\ln\left(\prod_i t_i\right) \frac{(\gamma_{eff} - \gamma_{tv})^{C_3}}{C_2} \tag{A. 6}$$

For Eq. (A. 3c), Eq. (A. 5b), and Eq. (A. 6), the parameter *t* plays a critical role in the model composition. Eq. (A. 3c) and Eq. (A. 5b) indicate that, besides shear cycles, the intermediate coefficient *t* determines the value of the model predicted volumetric strain increment ratio or volumetric strain ratio of any given shear cycles. As a result, laboratory test data of C_N vs. $n_{eq\gamma}$ should be usable for obtaining the regressed *t* values using Eq. (A. 5b).

In this thesis, the derived transformation equations have three major contributions. First, they disintegrate the complex iteration model into more specific expression forms, which reveals the model's implicated relationships among its contained variables and parameters. Secondly, different derived equations enable programing target-specified codes flexibly as shown in Appendix D. Relying on these codes, three calibration methods were established as presented in Appendix B. Lastly, connections between the Byrne model and the UCLA model were made, from which the coefficients back-calculation calibration method were developed (see details in Appendix C).

Appendix B: Methods of obtaining regressed coefficients

In this Appendix, three systematic methods were developed to obtain the regressed coefficients through MATLAB using the derived Byrne model equations. Method-related reusable codes were presented in Appendix D. These codes can be employed in either the Curve Fitting Toolbox or hand-written scripts. The Curve Fitting Toolbox is one built-in MATLAB application which can conduct curve fitting for either common models (e.g., linear, polynomial, power, and exponential) or customized models or functions. Compared with hand-written scripts, the Toolbox reflects more straightforward outcomes, so the subsequent discussions only took the Toolbox curve fitting results as examples. Additionally, for the convenience of presentation, the best fit prediction corresponded C_1, C_2, and C_3 were named as best-fitting C-coefficients, among which C_1 and C_2 were named as best-fitting C-pair.

In accordance with different presenting ways, the regression used published test data can be classified into three categories: (1) Type 1 data display test results in a form of ε_v vs. $n_{eq\gamma}$ under given γ_{eff} (e.g., Figure B.1); (2) Type 2 data exhibit test result in a form of C_N vs. $n_{eq\gamma}$ (e.g., Figure B.2); (3) Type 3 data present test result in a form of $\varepsilon_{v,15}$ vs. γ_{eff} (e.g., Figure B.3). As discussed in Appendix A, the Byrne (1991) model can utilize Eq. (A. 4c) and Eq. (A. 5a) to characterize relations of $\varepsilon_{v,15}$ vs. γ_{eff} and C_N vs. $n_{eq\gamma}$ respectively. Accordingly, Eq. (A. 4c) was coded in MTALAB to perform regression based on Type 3 data, and Eq. (A. 5a) was coded as the MATLAB function "N_VS_Nor_V" (see Appendix D) to perform regression based on Type 2 data.

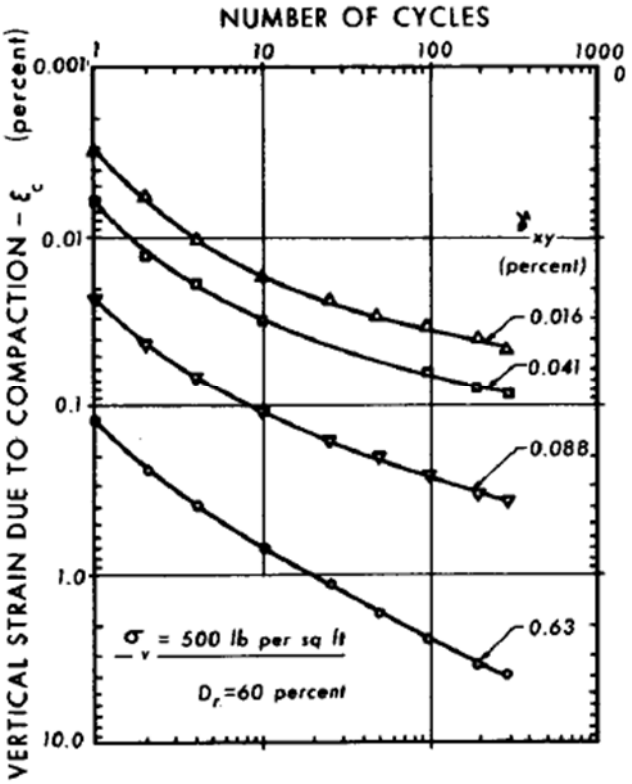

Figure B.1: Type 1 data example of ε_v vs. $n_{eq\gamma}$ under given γ_{eff} (Silver and Seed, 1971)

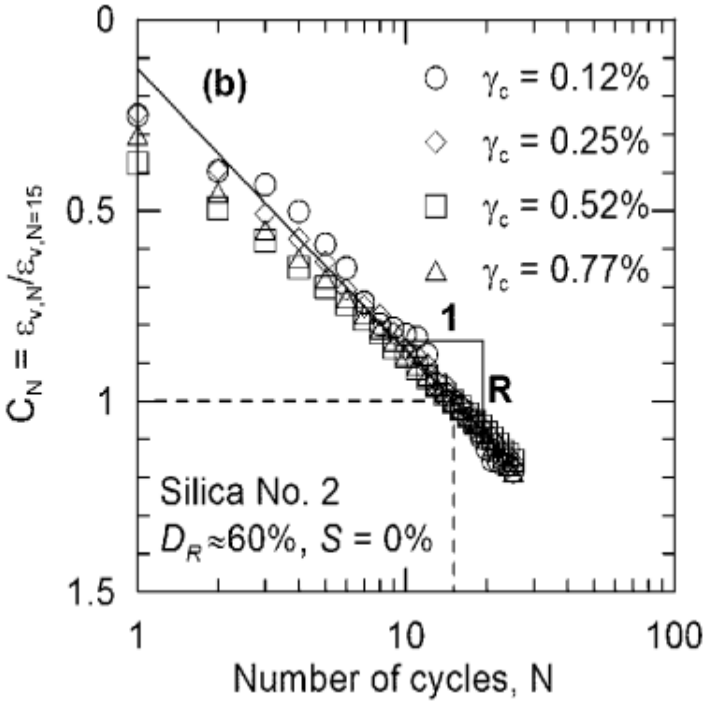

Figure B.2: Type 2 data example of C_N vs. $n_{eq\gamma}$ (Duku et al., 2008)

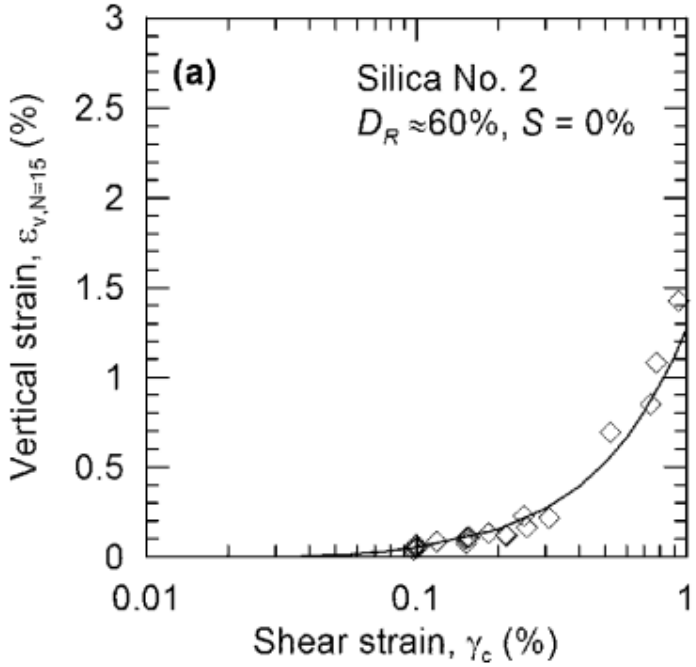

Figure B.3: Type 3 data example of $\varepsilon_{v,15}$ vs. γ_{eff} (Duku et al., 2008)

Doing regression for Type 1 data is the most effortless way to reach the best-fitting C-coefficients. The regression used model can be Eq. (8a) or Eq. (8b). However, few Type 1 data were available in the published literature. Whereas, plenty of Type 2 or 3 data can be found in papers (e.g., Whang 2001; Stewart et al. 2004b; Duku et al. 2008; Yee et al. 2014). However, Eq. (8a) or Eq. (8b) are not suitable for Type 2 or 3 data regression. Therefore, to take full advantage of different types of data, the procedures for obtaining the best-fitting C-coefficients through the transformation equations were developed as presented follows.

1. Method 1: Obtaining the best-fitting C-pair based on Type 1 data

Method 1 was utilized to deal with single suite Type 1 data (ε_v vs. $n_{eq\gamma}$ under given γ_{eff}), where the functions "N_vs_V" and "N_half_vs_V" in Appendix D were employed in MATLAB as the customized models to execute the regression. To be specific, when doing regression in Curve Fitting Toolbox, it was required to import two column matrixes of $n_{eq\gamma}$ vs. ε_v in the Workspace window. These two matrixes were then selected as X and Y data in the Toolbox. Additionally, magnitude of shear strain γ_{eff} as well as threshold shear strain γ_{tv} need to be manually input into the self-defined function in the custom equation window. Another function input C_3 needs to specify its regression range (by clicking Fit Options) in the custom equation window or assign a given value (under this situation, Method 1 can only obtain the best-fitting C-pair), otherwise the Toolbox may not be able to return the regression results. The example of MATLAB regression results for Method 1 were shown in Figure B.4. As shown in Figure B.4, the input shear strain and threshold shear strain were 0.088 (%) and 0.01 (%) respectively,

and the assigned C_3 was 1. After regression, the best-fitting C-pair were $C_1 = 0.2472$ and $C_2 = 0.8807$.

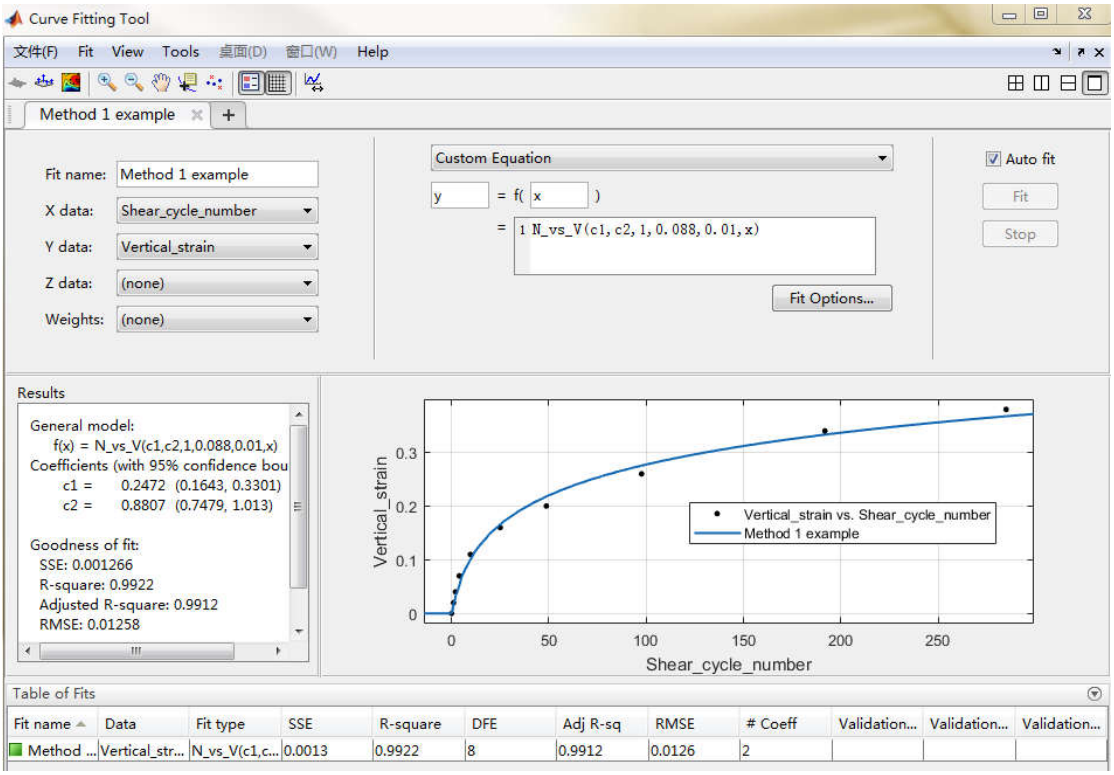

Figure B.4: Method 1 curve fitting screenshot example using Curve Fitting Toolbox (data from Silver and Seed, 1971)

The greatest advantage of Method 1 is it can get very accurate best-fitting C-pair for single set data without considering the dependency between C_1 and C_2. This is helpful to examine the potential C-pair dependency if adequate sets of Type 1 data were available. However, Method 1 is not compatible with doing regression by processing multi-suites of data simultaneously. This may lower data processing efficiency if generally suitable regression parameters were intended. Another disadvantage of Method 1 is its unstable performance of gaining the regressed C_3 when the assigned regression range of C_3 was large. To overcome these weaknesses in Method 1, Method 2 was developed.

2. Method 2: Obtaining the best-fitting C-coefficients by means of 3-D curve fitting

Method 2 performs data regression by using a MATLAB function called "Three_D_fitting" as presented in Appendix D. Multi-suites of test data can be handled by Method 2 at the same time as long as the regressed data include enough number of ε_v with its corresponding $n_{eq\gamma}$ and γ_{eff} (e.g., Figure B.1 and Figure B.5). When doing regression in Curve Fitting Toolbox, it was required to import three column matrixes of ε_v, $n_{eq\gamma}$, and γ_{eff} in the Workspace window. These three matrixes were selected as X, Y

and Z data in the Toolbox. After then, the Toolbox would generate points in a 3-D space with three axis representing $n_{eq\gamma}$, γ_{eff}, and ε_v as shown in Figure B.5. Since the regression was achieved in a 3-D space, Method 2 was also named as 3-D curve fitting method in this thesis. Unlike Method 1 which finally gained one best fitted curve in a 2-D space, Method 2 was trying to find the best fitted curved surface in a 3-D space (see Figure B.7). When using the Toolbox, before regression, it was required to manually input the known threshold shear strain into the self-defined function in the custom equation window. Figure B.8 was the screenshot of Curve Fitting Toolbox as an example of the Method 2 regression results. In Figure B.8, the best-fitting C-coefficients were $C_1 = 0.1527$, $C_2 = 0.4746$, and $C_3 = 1.1$ and a 0.01% threshold shear strain was assigned.

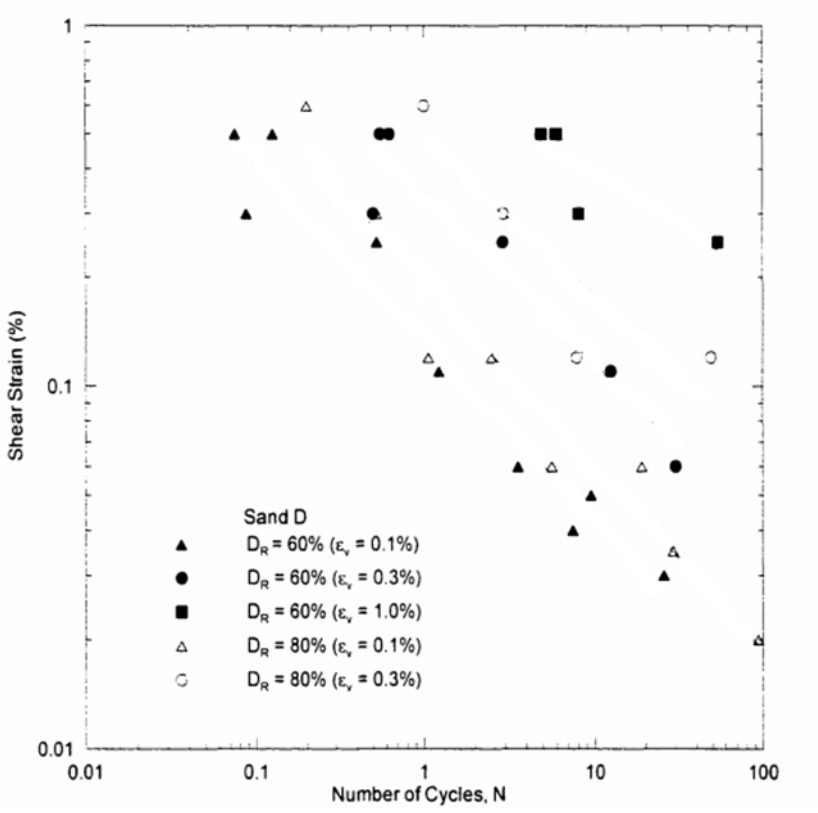

Figure B.5: Example of test data (Whang, 2001) that can be processed by Method 2

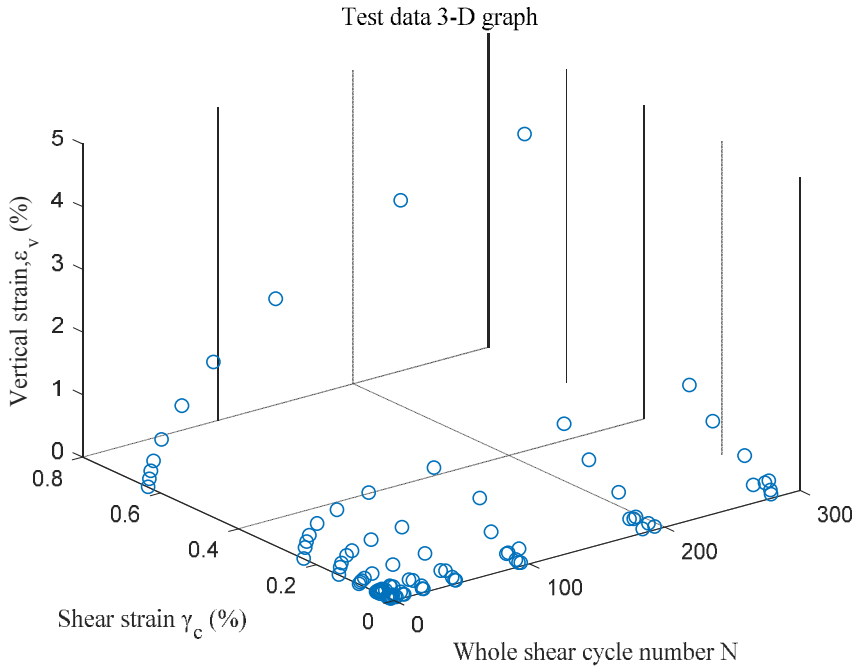

Figure B.6: Curve Fitting Toolbox generated test data points in a 3-D space (data from Silver and Seed, 1971)

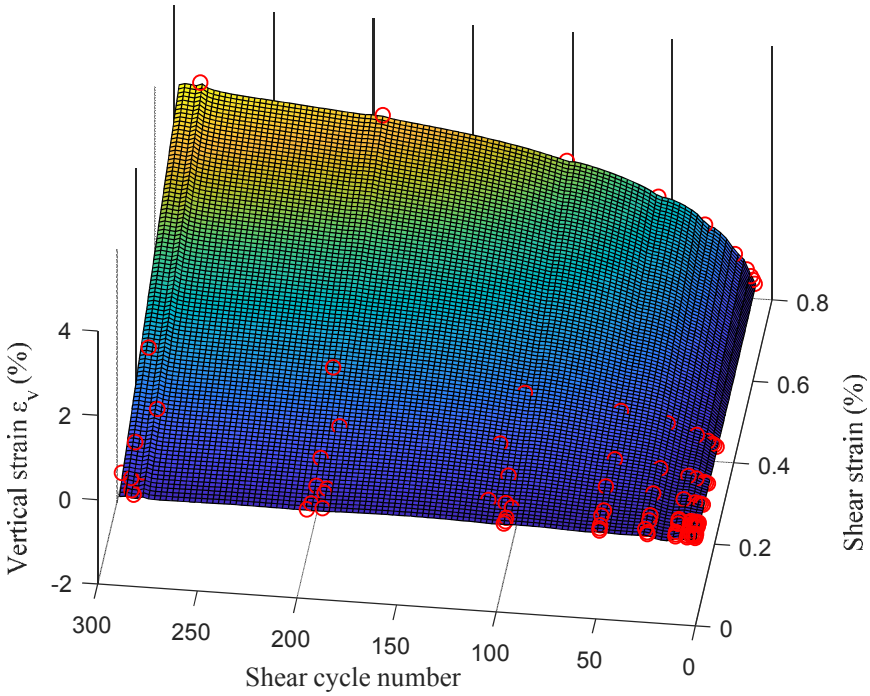

Figure B.7: Method 2 best fitted curved surface in 3-D space (data from Silver and Seed, 1971)

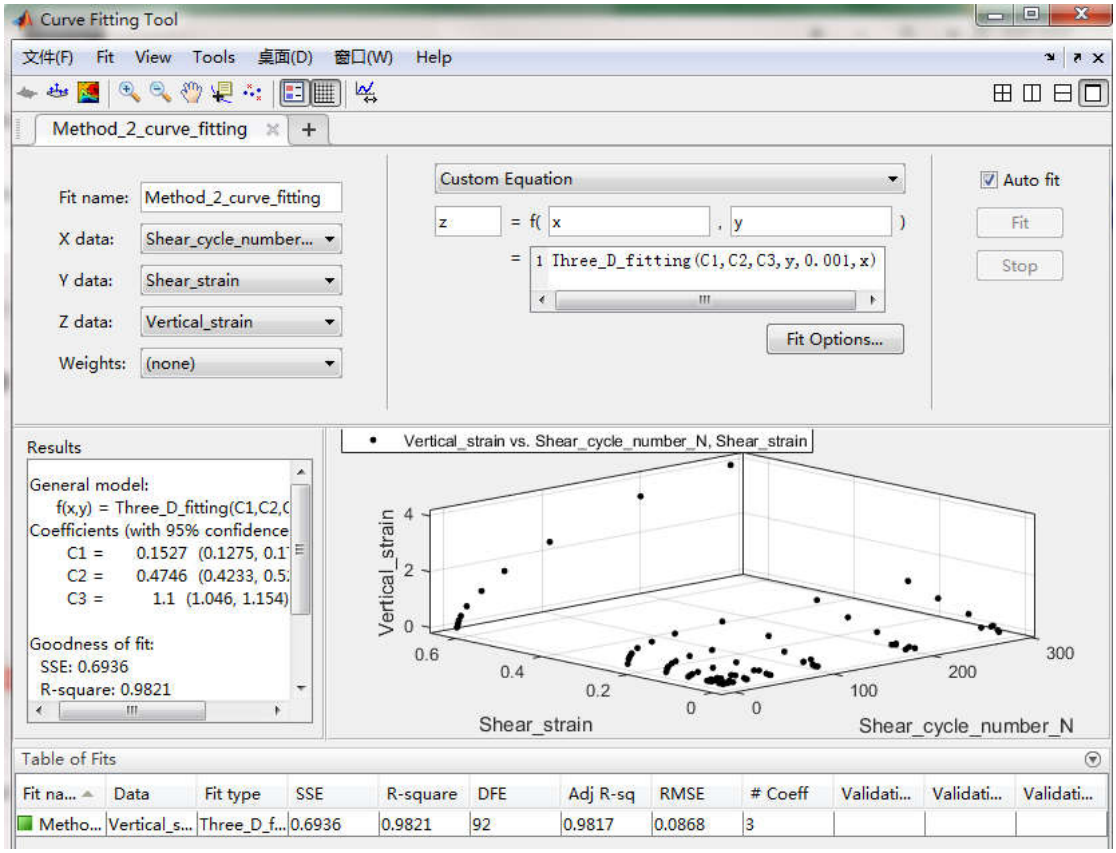

Figure B.8: Method 2 curve fitting result screenshot example of Curve Fitting Toolbox (data from Silver and Seed, 1971)

In contrast with Method 1, Method 2 can deal with groups of test data at the same time, which offers efficient way to determine generally applicable C-coefficients including C_3. More importantly, Method 2 can completely substitute Method 1 with better regression performance in terms of processing Type 1 data. To process Type 1 data, besides importing matrixes of $n_{eq\gamma}$ and ε_v, Method 2 needs to create matrix of γ_{eff} in the Workspace window as the selected Z data in the Toolbox. Specifically, for handing same Type 1 data, if identical C_3 was assigned in the self-defined functions of Method 1 and Method 2, the two methods will return same regression results. Overall, Method 2 is more practical and efficient than Method 1. Accordingly, when test data are enough and detailed, it is highly recommended performing 3-D curve fitting for obtaining best-fitting C-coefficients.

3. Method 3: Obtaining the best-fitting C-coefficients based on Type 2 and Type 3 data

Method 3 was employed to process the Type 2 and Type 3 data. Only one set of test data can be processed by method 3 every time. Unlike Method 1 and Method 2, Method

3 not only conducted regression, but also executed analytical calculations. Method 3 included three steps.

The first step was performing Type 2 data regression by using a MATLAB function "N_VS_Nor_V". Matrixes of $n_{eq\gamma}$ and C_N were needed to be imported into the Workspace window. These two matrixes were then selected as X and Y data in the Toolbox. Before regression, it was required to assign a random shear strain value into the self-defined function. Otherwise, the curve fitting could not be completed successfully. (Note that the randomly assigned shear strain will not impact the regression results). One example of Type 2 data regression was shown in Figure B. 9, where the returned C-coefficients were $C_1 = 0.7547$ and $C_2 = 0.5569$ separately. Note that the obtained C_1 or C_2 here was not the "true" best-fitting C_1 or C_2 for the Byrne model. They were merely two random figures that had certain constant arithmetic product. Through analysis of Eq. (A. 5b), it was easy to find such constant product was exactly the best-fitting C-pair product *P*, because "N_VS_Nor_V" was coded based on Eq. (A. 5b) where only parameter *t* (or *P*) were the regressed coefficient. Hence, one critical usage of "N_VS_Nor_V" is obtaining the best fitting C-pair product *P* (or parameter *t*). As a result, the inherent regressed results in Figure 2.10 should be $P = 0.420$ or $t = 0.811$.

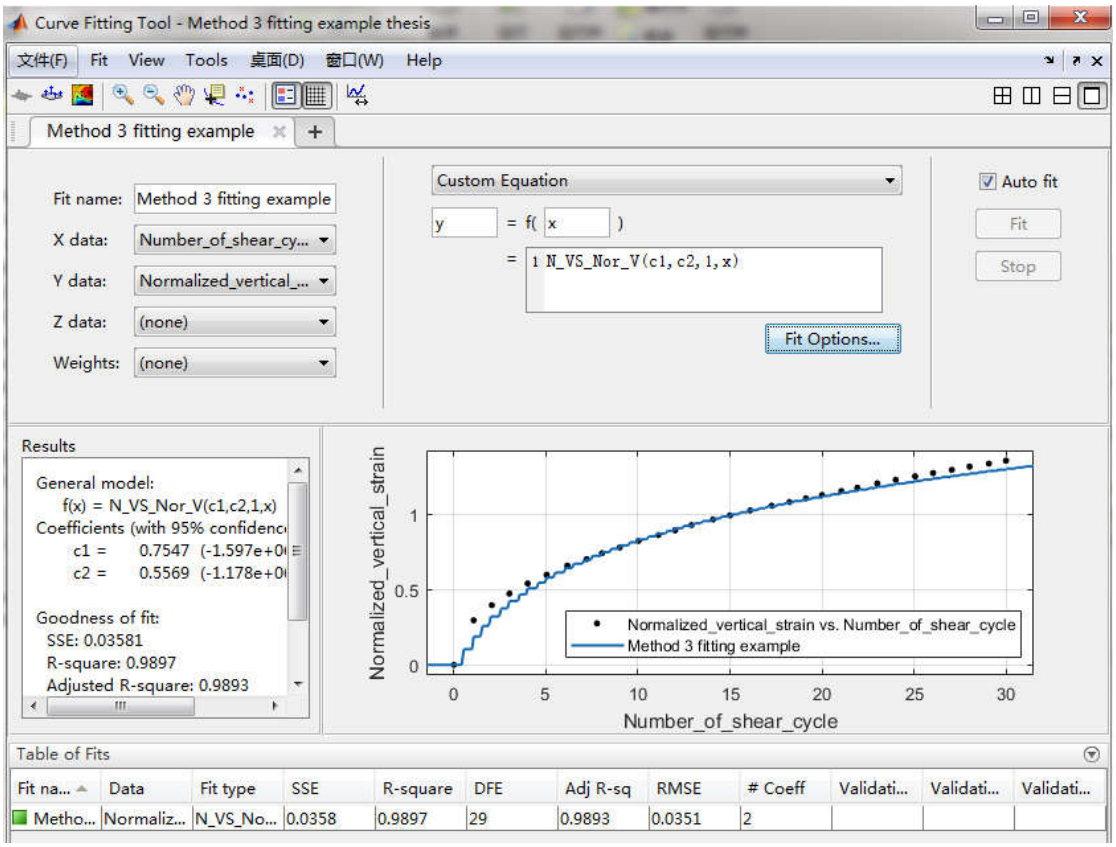

Figure B.9: Type 2 data curve fitting example of Method 3: screenshot of Curve Fitting Toolbox (data from Whang, 2001)

The second step of Method 3 was executing regression for Type 3 data by using customized equation $y = ax^b$. Before regression, matrixes of $(\gamma_{eff} - \gamma_{tv})$ and $\varepsilon_{v,15}$ were needed to be imported in the Workspace window and then selected as X and Y data in the Toolbox. The coefficients a and b in the customized equation are corresponded to the item $-\ln(\prod_i t_i)/C_2$ and the exponential item C_3 in Eq. (A. 6), so the regression coefficients a and b here were in reality the regressed $-\ln(\prod_i t_i)/C_2$ and C_3. Example of Type 3 data regression using $y = ax^b$ was shown in Figure B.10, from which $a = -\ln(\prod_i t_i)/C_2 = 1.703$ and $b = C_3 = 1.092$.

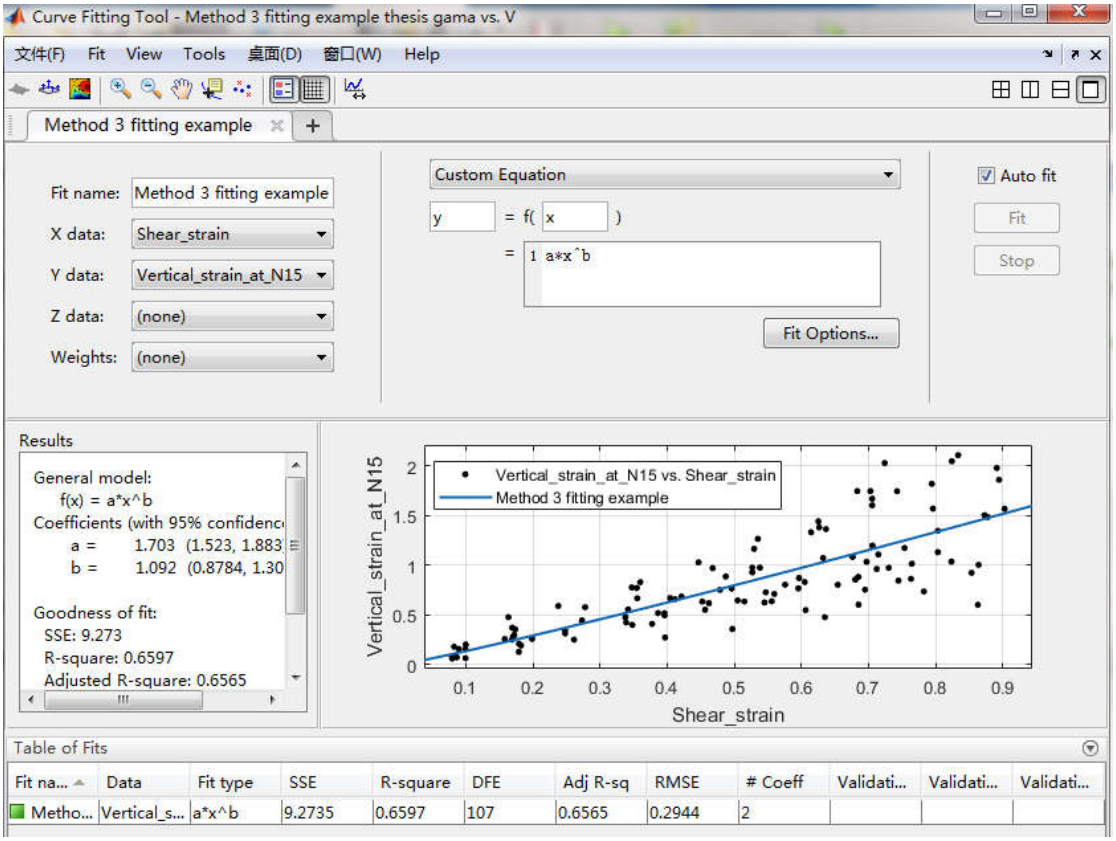

Figure B.10: Type 3 data curve fitting example of Method 3: screenshot of Curve Fitting Toolbox (data from Stewart et al., 2004b)

The last step of Method 3 was back calculating the best-fitting C-coefficients. Input the regressed value of *t* (or *P*) into $-\ln(\prod_i t_i)/C_2$, C_2 was able to be solved. Note this C_2 should be the best-fitting prediction corresponded coefficient. Then, using the *P* value known from the first step, it is easy to back calculate the best-fitting C_1.

4. Regression analysis for currently available published data

Even though three different methods were established for obtaining regressed C-coefficients, few published Type 1 data were available for Method 1 or Method 2 analysis. While numerous Type 3 data were available in papers, lacking specific Type 2 data from the papers makes Method 3 unable to gain the best fitting C-pair. Hence, to

investigate the potential coefficient dependency or to update the coefficient correlations was not easy based on existing usable data. Even so, this study still gained some findings from the currently available regression results.

Because the data from Silver and Seed (1971) were detailed and easy to digitize, using their data, a series of Method 1 regression (assuming $\gamma_{tv} = 0$ and $C_3 = 1$) were performed. The data details were presented in Figure B.11, where ten sets of cyclic shear test results were presented. To investigate the effect of the regression-considered shear cycle N scope on the best-fitting C-pair, regressions were executed for data points with N ranges from 0-10, 0-25, 0-100, and 0-280 respectively. The regression results were summarized in Table B.1. The goodness of fit criteria used in this study was the sum of squares due to error (SSE). A small SSE denotes a tight fit of the model to the data.

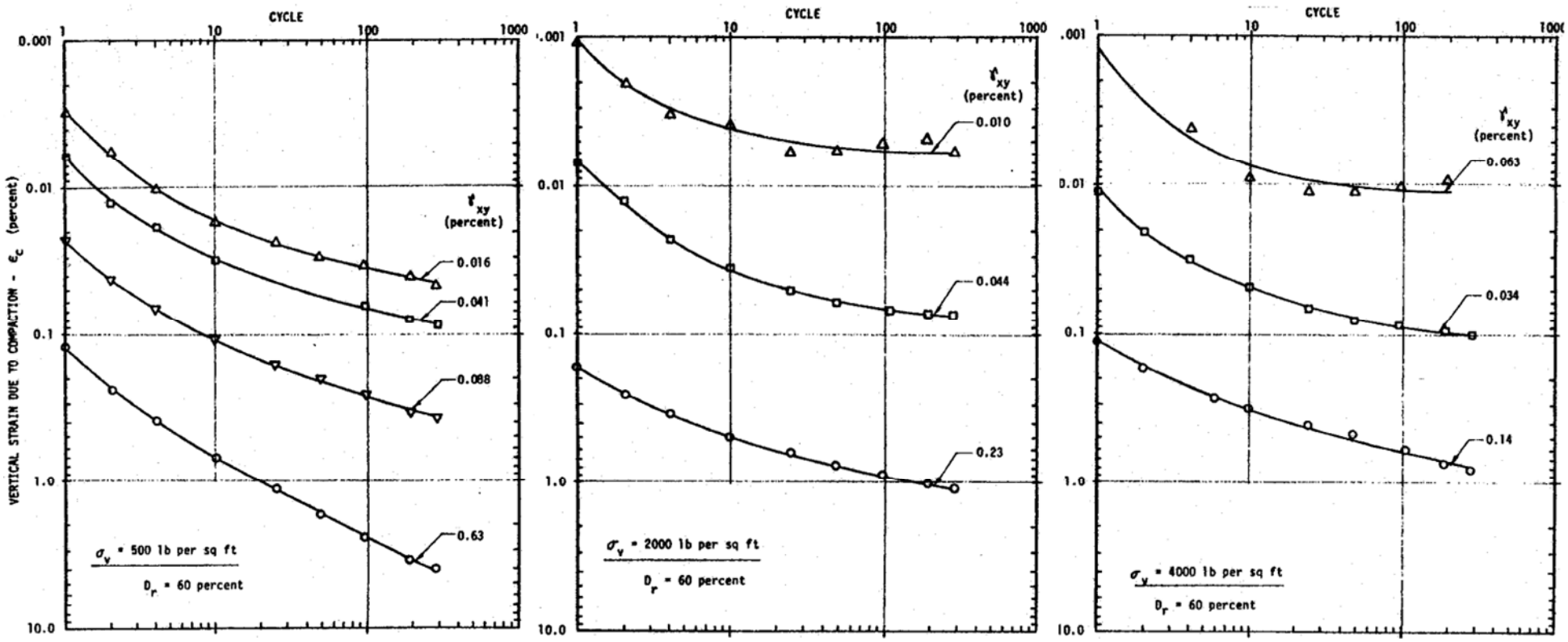

Figure B.11: Ten sets of stain-controlled cyclic direct simple shear test for D_r = 60% clean sand (Silver and Seed, 1971)

Table B.1: The regressed C_1 and C_2 with corresponding values of *t*, *P*, and SSE for data of Silver and Seed (1971)

Test information				For test points of $0 \leq N \leq 10$					For test points of $0 \leq N \leq 25$					For test points of $0 \leq N \leq 100$					For test points of $0 \leq N \leq 280$				
Test suite #	σ_v (psf)	D_r(%)	γ(%)	C_1	C_2	*t*	*P*	SSE	C_1	C_2	*t*	*P*	SSE	C_1	C_2	*t*	*P*	SSE	C_1	C_2	*t*	*P*	SSE
1	**500**	**60**	**0.02**	**0.23**	**1.26**	**-0.14**	**0.865**	**4E-07**	**0.26**	**1.59**	**-0.205**	**0.815**	**2E-06**	**0.28**	**1.76**	**-0.249**	**0.780**	**3E-06**	**0.28**	**1.73**	**-0.239**	**0.787**	**8E-06**
2	**500**	**60**	**0.04**	**0.18**	**2.02**	**-0.19**	**0.831**	**1E-06**	-	-	-	-	-	**0.21**	**2.48**	**-0.258**	**0.773**	**4E-06**	**0.19**	**2.29**	**-0.221**	**0.802**	**1E-05**
3	**500**	**60**	**0.09**	**0.31**	**1.21**	**-0.19**	**0.830**	**8E-05**	**0.33**	**1.38**	**-0.225**	**0.799**	**1E-04**	**0.30**	**1.27**	**-0.190**	**0.827**	**2E-04**	**0.22**	**0.99**	**-0.109**	**0.897**	**1E-03**
4	**500**	**60**	**0.63**	**0.21**	**1.06**	**-0.11**	**0.893**	**2E-04**	**0.21**	**1.03**	**-0.110**	**0.896**	**2E-04**	**0.14**	**0.57**	**-0.041**	**0.960**	**3E-02**	**0.11**	**0.42**	**-0.024**	**0.977**	**7E-02**
5	**2000**	**60**	**0.01**	**0.25**	**8.52**	**-1.06**	**0.347**	**3E-07**	**0.13**	**4.75**	**-0.306**	**0.736**	**3E-07**	**0.30**	**9.15**	**-1.359**	**0.257**	**3E-06**	**0.35**	**11.27**	**-1.972**	**0.139**	**7E-06**
6	**2000**	**60**	**0.04**	**0.19**	**1.80**	**-0.17**	**0.845**	**2E-06**	**0.20**	**2.10**	**-0.213**	**0.808**	**5E-06**	**0.25**	**2.60**	**-0.322**	**0.725**	**3E-05**	**0.31**	**3.11**	**-0.487**	**0.614**	**1E-04**
7	**2000**	**60**	**0.23**	**0.93**	**1.14**	**-0.53**	**0.590**	**6E-05**	**1.00**	**1.24**	**-0.618**	**0.539**	**4E-04**	**0.99**	**1.24**	**-0.614**	**0.541**	**5E-04**	**0.98**	**1.23**	**-0.602**	**0.548**	**5E-04**
8	**4000**	**60**	**0.01**	**0.32**	**1.16**	**-0.18**	**0.832**	**2E-06**	**0.31**	**1.33**	**-0.208**	**0.812**	**2E-06**	**1.07**	**2.96**	**-1.585**	**0.205**	**1E-05**	**1.70**	**3.71**	**-3.163**	**0.042**	**2E-05**
9	**4000**	**60**	**0.03**	**0.46**	**1.39**	**-0.32**	**0.728**	**1E-05**	**0.47**	**1.45**	**-0.342**	**0.710**	**1E-05**	**0.53**	**1.64**	**-0.437**	**0.646**	**5E-05**	**0.63**	**1.84**	**-0.578**	**0.561**	**1E-04**
10	**4000**	**60**	**0.14**	**1.61**	**1.38**	**-1.11**	**0.330**	**8E-06**	**1.58**	**1.35**	**-1.063**	**0.345**	**5E-05**	**1.44**	**1.25**	**-0.904**	**0.405**	**1E-03**	**1.00**	**1.01**	**-0.505**	**0.604**	**1E-02**

Using the best-fitting C-pairs in table B.1, Figure B.12 were drawn to analyze the possible dependency between C_1 and C_2. Given the Byrne (1991) recommended $C_1 = 0.4/C_2$ in the original model, an inverse proportion relation of C-coefficients was examined by a customized equation $C_1 = P/C_2$ in the Curve Fitting Toolbox. After the regression for all points in Figure 2.13, $P = 0.52$ with $SSE = 217$ was gained. Then, excluding some possible outlier-points in figure B.13, the Toolbox gained $P = 0.37$ with $SSE = 28$. Both 0.52 and 0.37 were close to 0.4. Since Byrne (1991) proposed $C_1 = 0.4/C_2$ based on data from Silver and Seed (1971), the results verified the reasonability of the Byrne's suggestion. However, scattered C_1 vs. C_2 points resulted in very large SSE values of the fit, plus only ten suites of test results were regressed, so it was hard to determine if the inverse proportion C-pair dependency was generally suitable. Since no other apparent dependency can be found in Figure B.12, the scattered C_1 vs. C_2 may also implicate that the C-pair were not inter-dependent. If this was the case, current available published data would be far more enough to calibrate the model coefficients. All in all, no matter how C-pair is dependent or not, to get more definitive conclusion on the coefficient dependency, adequate usable data are necessary. Otherwise, the model calibration can merely be achieved through alternative procedures instead of purely regression analysis.

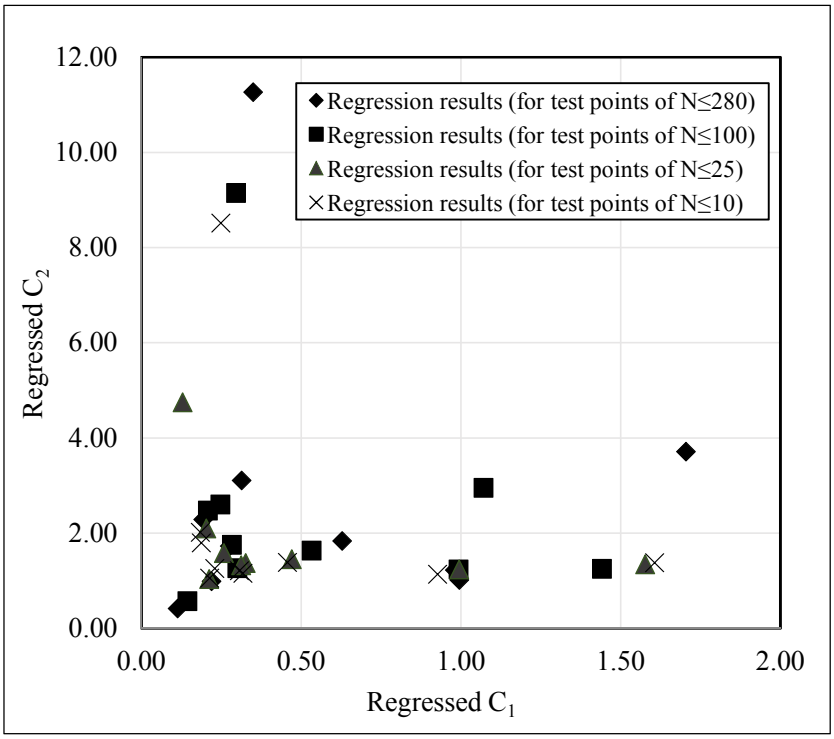

Figure B.12: Best-fitting C-pair for ten sets data with different considered N range

According to the results from Table B.12, Figure B.13, B.14, and B.15 were drawn to investigate the influence of considered N scope on regression results. Figure B.13 indicated that the increased considered N will increase the model prediction error or lower the model fit. This conclusion was suitable for all ten tests. In Figure B.14, it

seemed the varying regression-considered N can not significantly impact most of the regressed results, while only few sets of data showed significant regression difference due to the varying N. Additionally, the regression-considered N might affect the arithmetic product of best fitting C-pair as shown in Figure B.15. Due to the lack of adequate analyzed data, it was difficult to determine the definitive N influence on the regression results. Given the influence might be non-ignorable sometimes, this thesis suggested always mentioning the fitting-considered N scope before regression as a necessary precondition to calibrate the Byrne (1991) model.

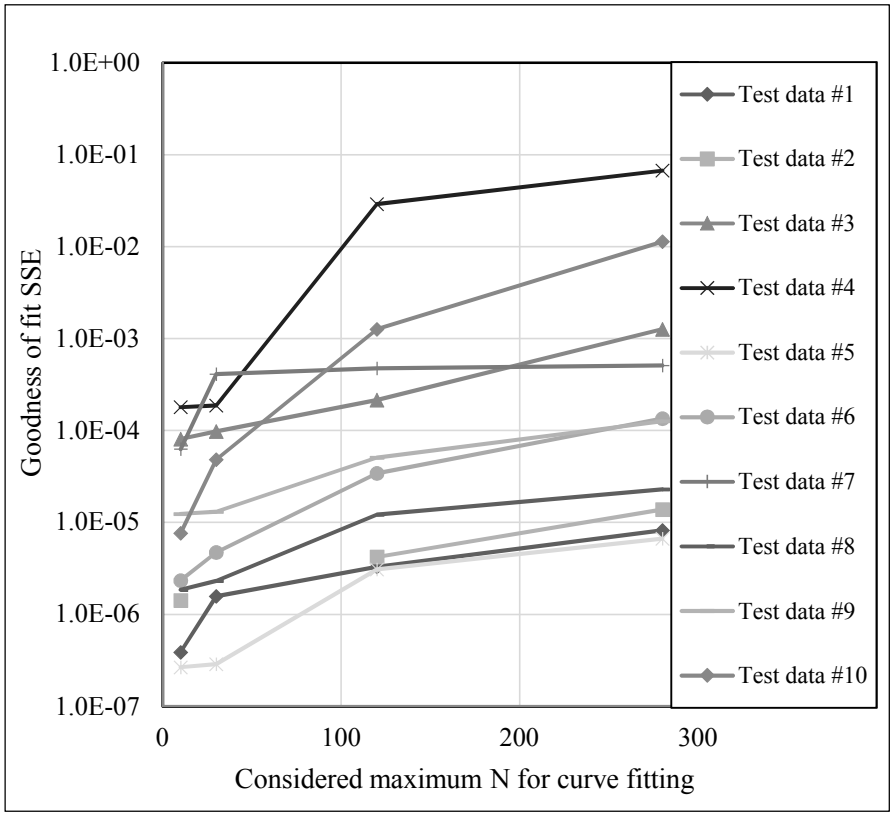

Figure B.13: Regression-considered N vs. SSE (data from Silver and Seed, 1971)

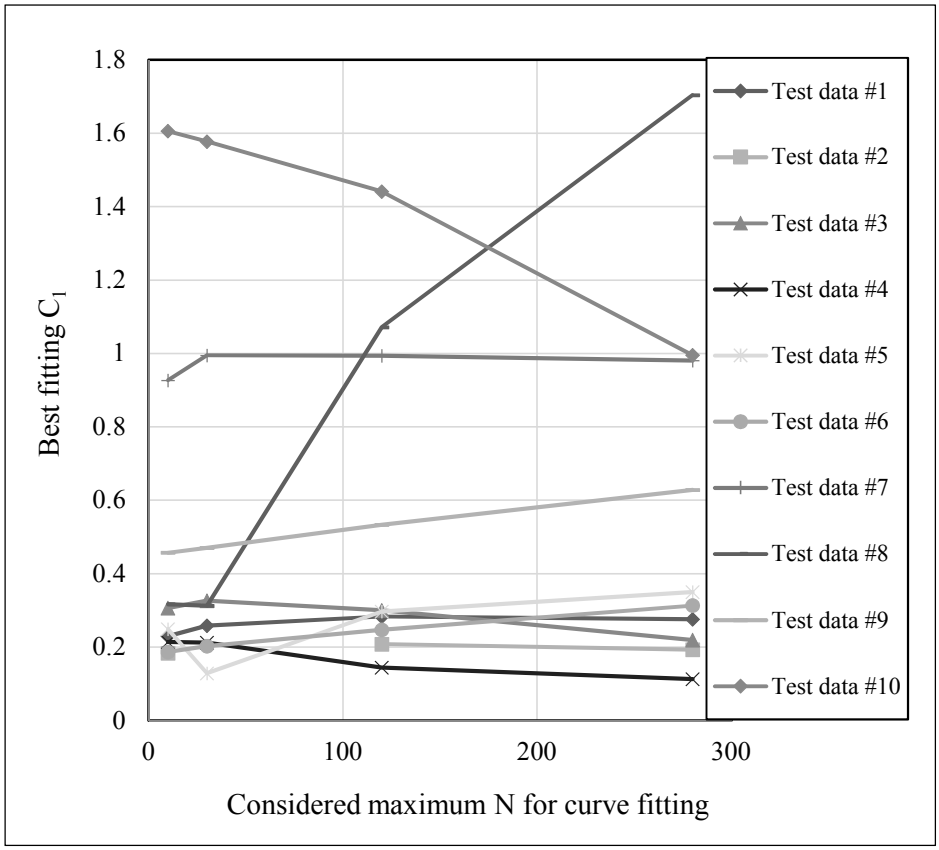

Figure B.14: Regression-considered N vs. best-fitting C_1 (data from Silver and Seed, 1971)

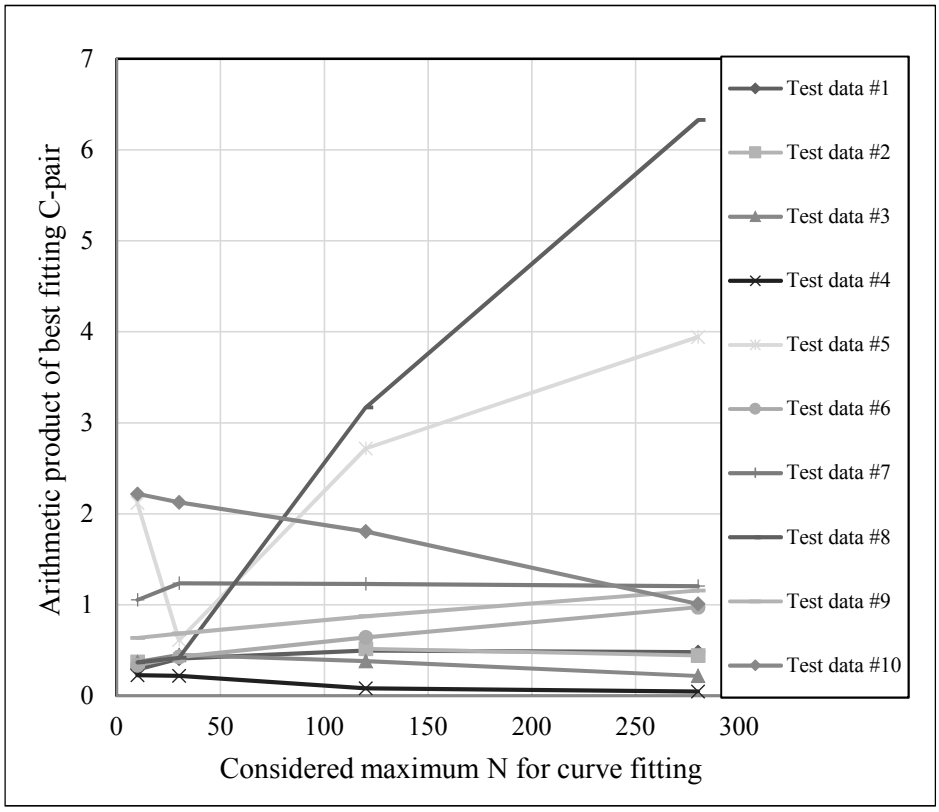

Figure B.15: Regression-considered N vs. best-fitting C-pair product (data from Silver and Seed, 1971)

Appendix C: Byrne model calibration based on the UCLA models

This Appendix presented the detailed Byrne model calibration based on the UCLA models as discussed in Section 2.4. From 2001 to 2014, researchers from UCLA conducted a large body of cyclic shear tests to investigate seismic compression, which greatly expanded the volumetric strain material model (VSMM) database (Yee et al., 2014). However, because this database was not published exhaustively, it was impossible to perform a robust regression for the Byrne (1991) model using the three developed methods as discussed in Appendix B. Whereas, regression results of the UCLA model were well-presented in the papers (e.g., Duku et al. 2008 and Yee et al. 2014). Through the transformed Byrne model equations, expression connections were found between the Byrne (1991) model and the UCLA model. Then the regressed Byrne model coefficients were back calculated via the UCLA models. As concluded at the end of Appendix B, it was necessary to mention the model regression considered shear cycle N. Since all the UCLA model regressed parameters were gained based on $0 \leq \mathrm{N} \leq 25$, such N scope was also applicable for the final calibrated Byrne models in this Appendix.

1. Calibrating C-pair product

Is it generally accepted C_N was mainly dependent on $n_{eq\gamma}$. For example, Tokimatsu and Seed (1987) used an empirical correlation table to describe C_N vs. $n_{eq\gamma}$ as shown in Table C.1; Pradel (1998) used equation $C_N = \left(n_{eq\gamma}/15\right)^{0.45}$ to represent how $n_{eq\gamma}$ affect C_N; Stewart et al. (2004b) concluded that the C_N vs. $n_{eq\gamma}$ exhibits little variability for 14 tested sands as shown in Figure C.1 and Duku et al. (2008) recommended using Eq. (2b) to describe a log-linear relation between C_N and $n_{eq\gamma}$ for clean sand. Similarly, as presented in Appendix A, the Byrne (1991) model can employed Eq. (A. 5b) to depict C_N vs. $n_{eq\gamma}$. In Eq. (A. 5b), constant t (or P) can be easily obtained by Method 3 regression using "N_VS_Nor_V", from which the calibration-desired C-pair dependency was indicated, because $t = e^{-0.5P}$ and $P = C_1 C_2$. This thesis accepted the assumption that C_N was primarily a function of $n_{eq\gamma}$ for clean sands, so C_1 and C_2 were interdependent with an inverse proportion relationship in the calibrated Byrne (1991) model. Then, the calibration of the C-pair product was achieved by C_N vs. $n_{eq\gamma}$ data regression. Note that for sand with fines of low plasticity, Yee et al. (2014) suggested C_N relies on both $n_{eq\gamma}$ and the shear strain γ_{eff}. As a result, to calibrate the C-pair product for the Byrne model of sand with fines, correlations among C_N , $n_{eq\gamma}$ and γ_{eff} were needed to be determined.

Table C.1: Empirical C_N vs. $n_{eq\gamma}$ relationship for clean sand (Tokimatsu and Seed, 1987)

Number of whole shear cycles, $n_{eq\gamma}$	Empirical C_N
26	0.89
15	1.0
10	1.13
5	1.32
2-3	1.5

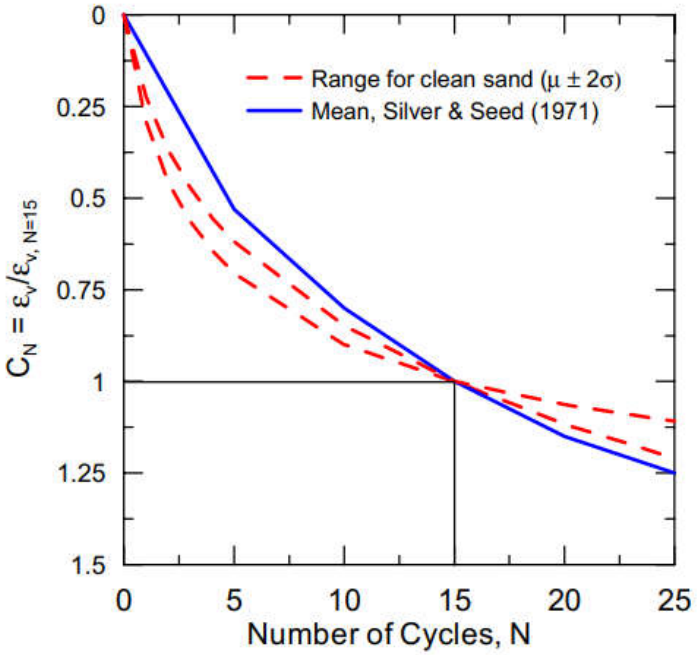

Figure C.1: C_N vs. $n_{eq\gamma}$ for the 14 tested clean sands (Stewart et al., 2004b)

2. Calibrating C-coefficients correlations

Both Eq. (A. 6) of the Byrne (1991) model and Eq. (2a) of the UCLA model utilized same power function expression form to describe $\varepsilon_{v,15}$ vs. γ_{eff}. The parameter *a* and *b* in Eq. (2a) was exactly corresponded to the item $-\ln(\prod_i t_i)/C_2$ and the exponential item C_3 in Eq. (A. 6). Hence, to obtain the equivalent regressed $-\ln(\prod_i t_i)/C_2$ and C_3 in the Byrne (1991) model, it was feasible to directly replace them with values of the regressed *a* and *b* from the UALC model. Via the replacement, the UCLA model coefficient correlations with various compositional and environmental factors can be transferred to the calibrated Byrne model, from which the C-coefficients correlation can be calibrated without performing regression analysis. In fact, gaining C_1 or C_2 through such equivalent coefficient back-calculation followed the same principles of Method 3 as discussed in Appendix B. The thorough processes of calibrating the Byrne (1991) model based on the UCLA model were presented in the following subsections,

where a calibrated Byrne model of clean sand and a calibrated Byrne model of sand with fines were proposed.

3. The calibrated Byrne model for clean sand based on the UCLA model regression results

Using the regressed results of the UCLA model of Duku et al. (2008), one calibrated Byrne model of clean sand was proposed in this section. Due to the paucity of detailed Type 2 data, this thesis had to use the UCLA model predicted C_N vs. $n_{eq\gamma}$ (ranging from 0 to 25) by Eq. (2b) to calibrate the C-pair product, where results of $P = 1$ and $t = 0.6035$ were gained. Therefore, in the Byrne model of clean sand, the updated C-pair dependency was $C_1 = 1/C_2$ as presented in Eq. (9b).

When $t = 0.6035$, Eq. (A. 6) can be written as $\varepsilon_{v,15} = 2.8001C_1 \times \left(\gamma_{eff} - \gamma_{tv}\right)^{C_3}$, within which $-\ln\left(\prod_i t_i\right)/C_2 = 2.8001\mathrm{C}_1$. Since Duku et al. (2008) suggested $a = (\sigma_v/P_a)^{-0.29}5.38e^{-0.023D_r}$ in their model, $2.8001C_1 = (\sigma_v/P_a)^{-0.29}5.38e^{-0.023D_r}$. By transposition, $C_1 = \frac{1}{2.8001} \cdot K_{\sigma,\varepsilon} \cdot a_{1\,atm} = \left(\frac{\sigma_v}{P_a}\right)^{-0.29} 1.92e^{-0.023D_r}$ as presented in Eq. (9a). Even though the regressed *b* was found varied with different materials, for the sake of developing a simplified model, Duku et al. (2008) recommended using constant $b = 1.2$ in their model. Given the regressed a expression were proposed based on $b = 1.2$, in the calibrated Byrne model, $\mathrm{C}_3 = b = 1.2$ was taken. In summary, the simplified form of the calibrated Byrne's model for clean sand can be written as:

$$\left(\Delta\varepsilon_{v,1/2}\right)_{i+1} = 0.5 \cdot \left(\gamma_{eff} - \gamma_{tv}\right)^{1.2} \cdot C_1 \cdot exp\left[-C_2 \frac{\varepsilon_{vi}}{\left(\gamma_{eff} - \gamma_{tv}\right)^{1.2}}\right] \qquad \text{(C. 1a)}$$

where $C_1 = (\sigma_v/P_a)^{-0.29}1.92e^{-0.023D_r}$ and $C_2 = 1/C_1$. Since C-coefficients are interdependent, Eq. (C. 1a) can be written as an one-coefficient expression:

$$\left(\Delta\varepsilon_{v,1/2}\right)_{i+1} = 0.5 \cdot \left(\gamma_{eff} - \gamma_{tv}\right)^{1.2} \cdot C_1 \cdot exp\left[-\frac{\varepsilon_{vi}}{C_1\left(\gamma_{eff} - \gamma_{tv}\right)^{1.2}}\right] \qquad \text{(C. 1b)}$$

Based on Eq. (C. 1b), a MATLAB function named "Calibrated_clean_sand_model" was coded, and the code details were presented in Appendix D. For the convenience of checking coefficient for the calibrated Byrne model of clean sand, Table C. 2 was proposed.

Table C.2: Calibrated model coefficient C_1 for clean sand with different relative density under different vertical load

σ_v (kPa)	Calibrated C_1 of the Byrne model								
	D_r=45%	D_r=50%	D_r=55%	D_r=60%	D_r=65%	D_r=70%	D_r=75%	D_r=80%	D_r=85%
50	0.83	0.74	0.66	0.59	0.53	0.47	0.42	0.37	0.33
75	0.74	0.66	0.59	0.53	0.47	0.42	0.37	0.33	0.30
100	0.68	0.61	0.54	0.48	0.43	0.38	0.34	0.30	0.27
125	0.64	0.57	0.51	0.45	0.40	0.36	0.32	0.29	0.25
150	0.61	0.54	0.48	0.43	0.38	0.34	0.30	0.27	0.24
*Coefficient calculation equation: $C_1 = \left(\frac{\sigma_v}{P_a}\right)^{-0.29} 1.92e^{-0.023D_r}$									

In the paper of Duku et al. (2008), the authors also presented material-specified regressed coefficients of the UCLA model as shown in Table C.3 (Note that in Table C.3, the coefficients were obtained when $K_{\sigma,\varepsilon} = 1$). Since the calibrated model of clean sand were broadly applicable for general clean sand, the model prediction may be biased when specific material was analyzed. Therefore, referring Table C.3 and following the same coefficient back-calculation procedures, similar material-specified coefficients table (Table C.4) was made for the calibrated Byrne model of clean sand.

Table C.3: UCLA model material-specified regression coefficients for tested clean sands (Duku et al., 2008)

		Column A		Column B
Material	D_R (%)	Intercept parameter a^*	Slope parameter b	Intercept parameter a^a
Vulcan	x45	2.65	1.16	2.55
	x60	1.73	1.21	1.71
	80	0.95	0.93	0.96
Silica No. 2	45	1.90	0.90	2.12
	x60	1.32	1.22	1.27
	x68	1.32	1.31	1.17
	x80	1.00	0.95	1.14
Crystal silica No. 30	60	1.14	0.68	1.58
F-52	x45	1.15	1.43	0.84
	x60	0.58	1.18	0.59
	x80	0.45	1.07	0.52
F-110	x60	1.74	1.46	1.29
Fint No. 13	60	1.31	0.95	1.46
Flint No. 16	60	1.76	1.05	1.85
Nevada	x60	1.43	0.97	1.65
	x80	1.27	1.46	0.98
Newhall	x60	1.21	1.23	1.18
Newhall No. 2	x45	1.19	1.23	1.17
	x60	0.75	1.43	0.63
Pacoima No. 1	60	1.70	0.95	1.89
Pacoima No. 3	60	1.47	0.99	1.64
Irwindale	60	1.32	0.98	1.38
Santa Clarita Post Office	60	0.83	0.91	0.92
Silica No. 0	60	1.74	1.13	1.42
Wilshire	x45	2.77	1.37	2.52
	x60	1.60	1.02	1.77
	x80	1.15	1.02	1.47

Note: x denotes test at a wide range of shear strains.

[a]Regression performed with slope parameter, $b=1.2$.

Table C.4: Byrne model material-specified calibration coefficients (for clean sand only)

-		Byrne model calibration coefficients		
Material	$D_r(\%)$	$\frac{C_1}{K_{\sigma,\varepsilon}}$	C_3	$\frac{C_1}{K_{\sigma,\varepsilon}}$ with $C_3 = 1.2$
Vulcan	[x]45	0.95	1.16	0.91
	[x]60	0.62	1.21	0.61
	80	0.34	0.93	0.34
Silica No.2	45	0.68	0.9	0.76
	[x]60	0.47	1.22	0.45
	[x]68	0.47	1.31	0.42
	[x]80	0.36	0.95	0.41
Crystal silica No. 30	60	0.41	0.68	0.56
F-52	[x]45	0.41	1.43	0.30
	[x]60	0.21	1.18	0.21
	[x]80	0.16	1.07	0.19
F-110	[x]60	0.62	1.46	0.46
Flint No.13	60	0.47	0.95	0.52
Flint No.16	60	0.63	1.05	0.66
Nevada	[x]60	0.51	0.97	0.59
	[x]80	0.45	1.46	0.35
Newhall	[x]60	0.43	1.23	0.42
Newhall No. 2	[x]45	0.42	1.23	0.42
	[x]60	0.27	1.43	0.22
Pacoima No.1	60	0.61	0.95	0.67
Pacoima No.3	60	0.52	0.99	0.59
Irwindale	60	0.47	0.98	0.49
Santa Clarita Post Office	60	0.30	0.91	0.33
Silica No.0	60	0.62	1.13	0.51
Wilshire	[x]45	0.99	1.37	0.90
	[x]60	0.57	1.02	0.63
	[x]80	0.41	1.02	0.53

Note: [x] denotes test at a wide range of shear strains

4. The calibrated Byrne model for sand with fines based on the UCLA model regression results

The calibrated Byrne model of sand with fines was proposed using the regressed results of the UCLA model of Yee et al. (2014). Note that both the UCLA model and the calibrated Byrne model of sand with fines discussed in this Appendix were suitable for non-plastic to moderately plastic silty sands/sandy silts (i.e., PI ≤ 10), with FC ranging from 0 to 60%..

In the UCLA model, the regression parameter *R* governs the predicted C_N vs. $n_{eq\gamma}$. Yee et al. (2014) found that *R* exhibited dependency on γ_{eff} and proposed the regressed Eq. (3d) to describe *R* vs. γ_{eff}. Using Eq. (3d) calculated results and following the same ways calibrating the C-pair product in the model of clean sand, values of *P* vs. *R* (the corresponding values of *R* ranging from 0.25 to 0.36) were regressed. Then, the plot of *R* vs. *P* was drawn as presented in Figure C. 2, where the regression expression was proposed:

$$R = -0.079\, ln(P) + 0.292 \tag{C. 2a}$$

Combing Eq. (3d) and Eq. (C. 2a), the C-pair product expression in the calibrated Byrne model for sand with fines were obtained:

$$P = e^{0.405}\left(\gamma_{eff} - \gamma_{tv}\right)^{0.3291} \tag{C. 2b}$$

According to Eq. (C. 2b), the updated C-pair dependency can be written as $C_1 = \frac{e^{0.405}\left(\gamma_{eff}-\gamma_{tv}\right)^{0.329\ 1}}{C_2}$.

Unlike the clean sand model calibration, for the sand with fine model, the C-coefficients correlation calibration was more complex due to the γ_{eff} dependent C-pair product. In the sand with fine model, because the item $-\ln\left(\prod_i t_i\right)/C_2$ in Eq. (A. 6) should equal to the item $K_{FC} \cdot K_S \cdot K_{\sigma,\varepsilon} \cdot a_{1\ atm\ \&\ FC=0\ \&\ S=0}$ in Eq. (3c), plus Eq. (C. 2b), following expression was gained:

$$K_{\sigma,\varepsilon} K_{FC}\ K_S 5.38 e^{-0.023 D_r} = \frac{-ln\left(\prod_{30} t_{30}\right)}{e^{0.405}\left(\gamma_{eff}-\gamma_{tv}\right)^{0.329\ 1}} \times C_1 \tag{C. 3a}$$

Since both *t* or *P* depends on γ_{eff}, the item $\frac{-ln\left(\prod_{30} t_{30}\right)}{e^{0.405}\left(\gamma_{eff}-\gamma_{tv}\right)^{0.329\ 1}}$ can be defined as a function of γ_{eff}, $F_P(\gamma_{\text{eff}})$. Then, C_1 can be written as:

$$C_1 = \frac{K_{\sigma,\varepsilon} K_{FC}\, K_S 5.38 e^{-0.023 D_r}}{F_P(\gamma_{eff})} \quad \text{(C. 3b)}$$

Because the expression of $F_P(\gamma_{eff})$ was too complicated, in order to efficiently calculate C_1 in Eq. (C. 3b), a simpler alterative $F_P(\gamma_{eff})$ expression was required. Hence, results of $F_P(\gamma_{eff})$ vs. γ_{eff} (varying from 0.03% to 1% with 0.01% increment) were calculated and then regressed by various self-defined equations. After trials, a simplified regressed expression regarding $F(\gamma)$ was proposed:

$$F_P(\gamma_{eff}) = 2.149 \gamma_{eff}^{-0.2343} + 4.337 e^{-66.56 \gamma_{eff}} \quad \text{(C. 4)}$$

Combining Eq. (C. 3b) and Eq. (C. 4), the equation of C_1 can be expressed as follows:

$$C_1 = \frac{K_{\sigma,\varepsilon} K_{FC}\, K_S 5.38 e^{-0.023 D_r}}{2.149 \gamma_{eff}^{-0.2343} + 4.337 e^{-66.56 \gamma_{eff}}} \quad \text{(C. 5)}$$

Eq. (C. 5) was the updated C-coefficient correlations in the calibrated Byrne model for sand with fines, where the influence of vertical load, fine content, degree of saturation, and soil density on seismic compression were all considered in it. Like Duku et al. (2008) suggested in the UCLA clean sand model, Yee et al. (2008) also recommended $b = 1.2$ in their model, so $C_3 = b = 1.2$ was accepted here as well.

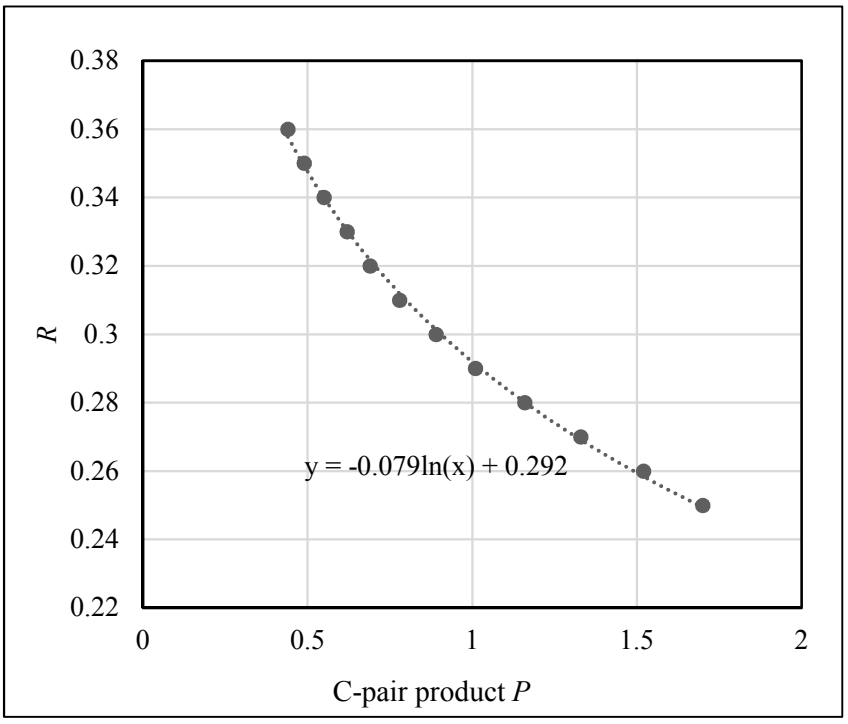

Figure C.2: Relationship of *R* and corresponding C-pair product *P*

In summary, the calibrated Byrne model for sand with fines of low plasticity is also expressed by Eq. (C. 1a). In contrast with the calibrated clean sand model, the calibrated sand with fine model has $C_1 = \frac{K_{\sigma,\varepsilon} K_{FC}\, K_S 5.38 e^{-0.023 D_r}}{2.149\gamma^{-0.2343} + 4.337 e^{-66.56\gamma}}$ and $C_2 = e^{0.405}(\gamma - \gamma_{tv})^{0.3291} / C_1$. The factor $K_{\sigma,\varepsilon}$, K_{FC}, and K_S within the model have same expression as Eq. (2d), Eq. (3a) , and Eq. (3b) of the UCLA model. Based on the calibrated Byrne model of sand with fines, the MATLAB function named "Calibrated_sand_with_fine_model" was coded. The details of the code were presented in Appendix D.

5. Threshold shear strain consideration in model calibration

Because the UCLA model coefficient *a* and *b* were regressed by equation $\varepsilon_{v,15} = a(\gamma_{eff} - \gamma_{tv})^b$, to perform the equivalent coefficient back-calculation for the Byrne model, one prerequisite should be the identical regression-based γ_{tv} between the two models. Otherwise, the calibrated C-coefficients in the Byrne model may not be the best fitting ones, especially when the γ_{eff} is very small. However, the detailed regression used γ_{tv} was not well-presented among the available literature from UCLA. In the thesis of Duku (2007), the author just mentioned a γ_{tv} scope of 0.01% to 0.02% for clean sand. In the paper of Duku et al. (2008), the authors indicated a typical clean sand γ_{tv} range of 0.01–0.03% by referring the conclusion of Hsu and Vucetic (2004). Whereas, for sand with fines, Duku (2007) did coefficient *a* regression with constant $b = 1.1$ using 0.02-0.03% γ_{tv}. In the thesis of Yee (2011), the author used various γ_{tv} values as shown in Table C.5 to perform the model regression. Hence, it is highly likely that the UCLA model coefficients were regressed based on non-unified γ_{tv} values. This might be insignificant, because the change of the small γ_{tv} values seems have negligible effect on the regression results. But to increase the Byrne model calibration accuracy, this thesis still recommended considering the influence of the γ_{tv} and mentioning the calibration used γ_{tv} clearly before any regression analysis.

Table C.5: The UCLA model regressed parameters with varied γ_{tv} values (Yee, 2011)

D_R	w	σ_v	a	b	γ_{tv}	a**
(%)	(%)	(kPa)			(%)	
32-43	6-7	100	1.91	1.34	0.03	1.88
28-42	17-18	50	2.50	1.11	0.038	2.56
31-41	17-19	100	2.27	1.33	0.034	2.23
33-43	17-18	200	1.86	1.42	0.03*	1.79
31-41	17-18	400	1.95	1.54	0.044	1.86
55-58	6-9	100	1.24	1.28	0.03*	1.22
56-67	16-17	100	1.42	1.33	0.03*	1.40
62-62	17-18	400	0.82	1.39	0.05*	0.63

6. Comparison between the Byrne (1991) model and the UCLA model

Compared with the original Byrne (1991) model, the UCLA model has better performance on characterizing $\varepsilon_{v,15}$ vs. γ_{eff}, because the original Byrne (1991) model only allowed a linear $\varepsilon_{v,15}$ vs. γ_{eff} prediction, whereas the UCLA model can perform a power law curve fitting. As discussed before, a curved fit line was more suitable than a straight fit line for most of the $\varepsilon_{v,15}$ vs. γ_{eff} test results. This can also be proved by Table C.4, where most of the regression parameter *b* was not 1 for different tested soils. Additionally, for same Type 3 data (see Figure C.3) from Silver and Seed (1971), the regression error comparison of the two models were presented in Table C.6. The comparison manifested that the UCLA model prediction can match the Type 3 data better. But after adding the third coefficient C_3, the Byrne model can also perform a power law curve fit for $\varepsilon_{v,15}$ vs. γ_{eff}. As a result, the expanded Byrne model has same prediction accuracy as well as calibration flexibility as the UCLA model in terms of depicting $\varepsilon_{v,15}$ vs. γ_{eff}.

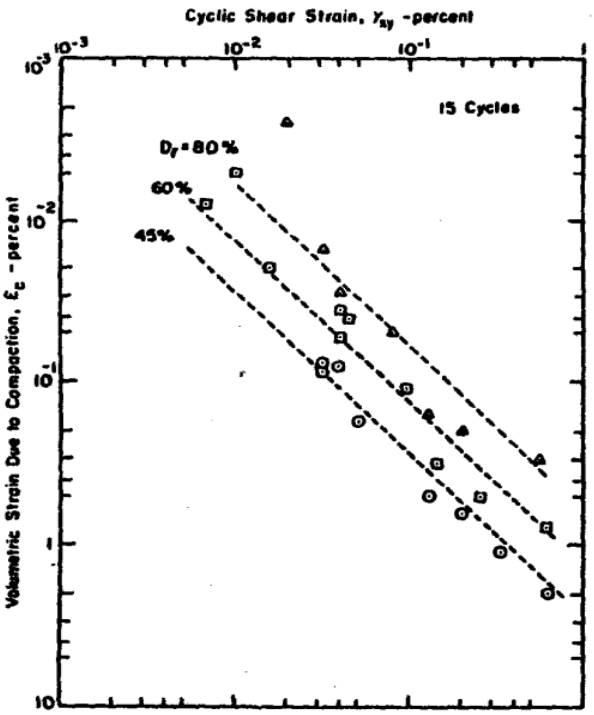

Figure C.3: Test data of $\varepsilon_{v,15}$ vs. γ_{eff} for different soil density by Silver and Seed (1971)

Table C.6: $\varepsilon_{v,15}$ vs. γ_{eff} prediction goodness of fit comparison between two models

Tested soil D_r (%)	SSE of the original Byrne (1991) model	SSE of the UCLA model
45	0.011	0.007
60	0.042	0.027
80	0.014	0.006

Unlike modifying the Byrne (1991) model expression form on describing $\varepsilon_{v,15}$ vs. γ_{eff}, this study did not adjust the model expression form on characterizing C_N vs. $n_{eq\gamma}$. This was because the Byrne (1991) model had more fit flexibility and less regression error than the UCAL model on C_N vs. $n_{eq\gamma}$ regression. Figure C. 4 presented the regression error for the two models employing same Type 2 data from Silver and Seed (1971). For the investigated eight sets of data, almost all SSE values of the Byrne (1991) model were smaller than those of the UCLA model. Also, it seems the SSE value difference for the two models were not obvious when the test shear strain was small. Since limited data were analyzed and the SSE difference of the two models was not apparent, the findings obtained from Figure C. 4 may not be broadly suitable. Given this, a more reliable model fit error comparison was carried out using data from Whang (2001), where average C_N vs. $n_{eq\gamma}$ (See Figure C. 5) of 4 sands with more than 40 suites of tests were regressed. Figure C. 6 showed the SSE histogram comparison between the two models, where the Byrne (1991) model showed far less SSE values than the UCLA model for the 4 sands. This proved that the Byrne (1991) model has better regression performance on C_N vs. $n_{eq\gamma}$. More importantly, the near 0 SSE values implies a great fit capability of the Byrne (1991) model on Type 2 data regression.

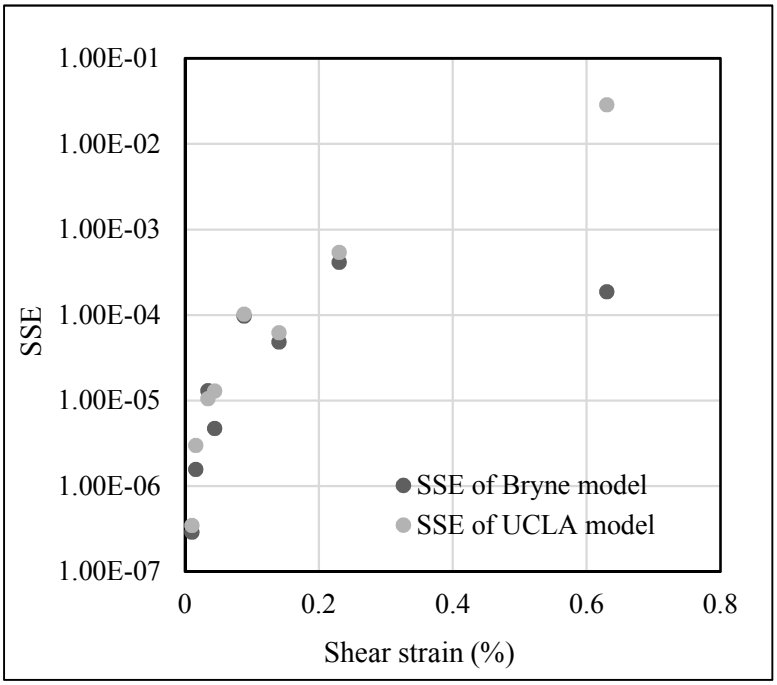

Figure C.4: C_N vs. $n_{eq\gamma}$ data of Silver and Seed (1971) regression results

comparison between the Byrne (1991) model and the UCLA model

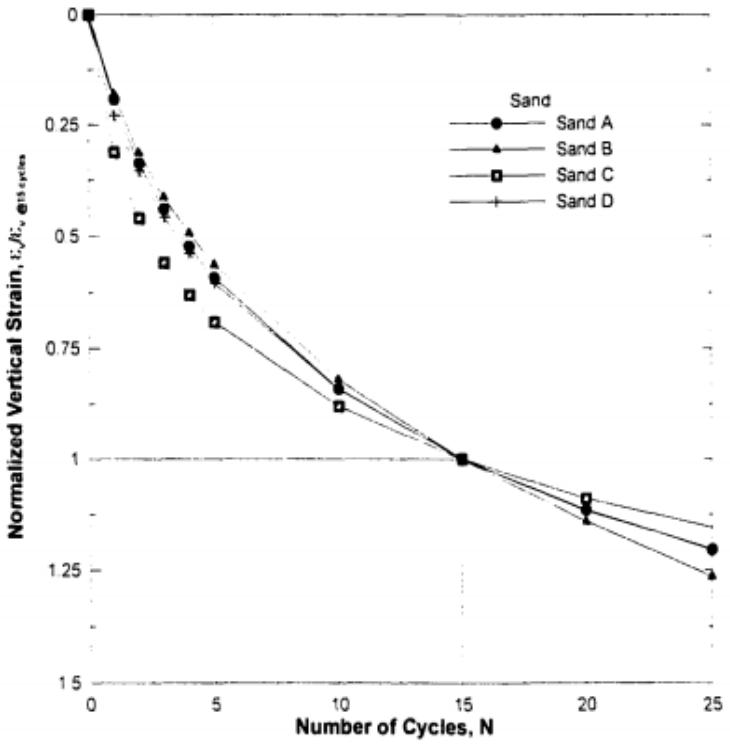

Figure C.5: Average C_N vs. $n_{eq\gamma}$ for 4 sands with more than 40 laboratory tests (Whang, 2001)

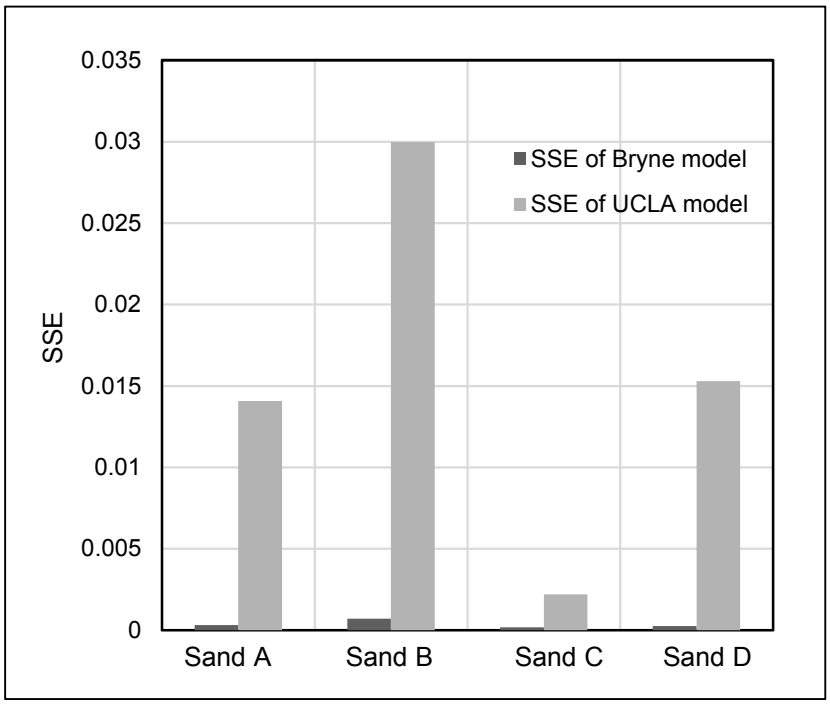

Figure C.6: Regression SSE comparison between the Byrne (1991) model and the UCLA model using average C_N vs. $n_{eq\gamma}$ of 4 sands (data from Whang,

2001)

Even though the Byrne (1991) model can better characterize C_N vs. $n_{eq\gamma}$ than the UCLA model, it should be noted that this study did not give full play to such advantage on the model calibration. Because of the paucity of the C_N vs. $n_{eq\gamma}$ data, this thesis had to use the UCLA model predicted C_N vs. $n_{eq\gamma}$ to perform the regression and then obtained the calibrated C-pair product. Figure C. 7 was drawn to compare the predicted C_N vs. $n_{eq\gamma}$ among the UCLA model (Duku et al, 2008) with $R = 0.29$, the original Byrne (1991) model with $P = 0.4$, and the calibrated Byrne model of clean sand with $P = 1$. As shown in Figure C. 7, compared with the original Byrne (1991) model, the calibrated model of clean sand had larger predicted C_N at $n_{eq\gamma} = 1$ to 14 but smaller predicted C_N at $n_{eq\gamma} = 16$ to 25. Additionally, in Figure C. 7, the Byrne (1991) model still exhibited excellent C_N vs. $n_{eq\gamma}$ regression performance that even the UCLA model predicted points were perfectly fitted. However, since *P* was not calibrated utilizing the real test data, it was hard to know whether the updated C_N vs. $n_{eq\gamma}$ prediction was more accurate than before. Given the two models can characterize almost same C_N vs. $n_{eq\gamma}$ as well as identical $\varepsilon_{v,15}$ vs. γ_{eff}, the calibrated Byrne model was basically equivalent to the UCLA model. Even so, this thesis believed that as along as enough test data were available, the calibrated Byrne model will still be overall more accurate and efficient than the UCLA model in seismic compression evaluation. The higher accuracy of the Byrne model lies in its better regression capability on C_N vs. $n_{eq\gamma}$. Whereas, the higher efficiency of the Byrne model comes from it has less regression coefficients (C_1, C_2 and C_3) than the UCLA model. Especially when considering interdependent C-pair and $C_3 = 1.2$, merely one coefficient will be involved in the model calibration. In contrast, the UCLA model has four parameters (*R*, *c*, *a*, and *b*) in its expression. Assuming $b = 1.2$ and *c* can be back calculated from $1 - Rln(15)$, the UCLA model still requires at least two coefficients (*R* and *a*). More importantly, the calibrated Byrne model can also be used in non-simplified analysis, but the UCLA model is merely suitable for simplified analysis.

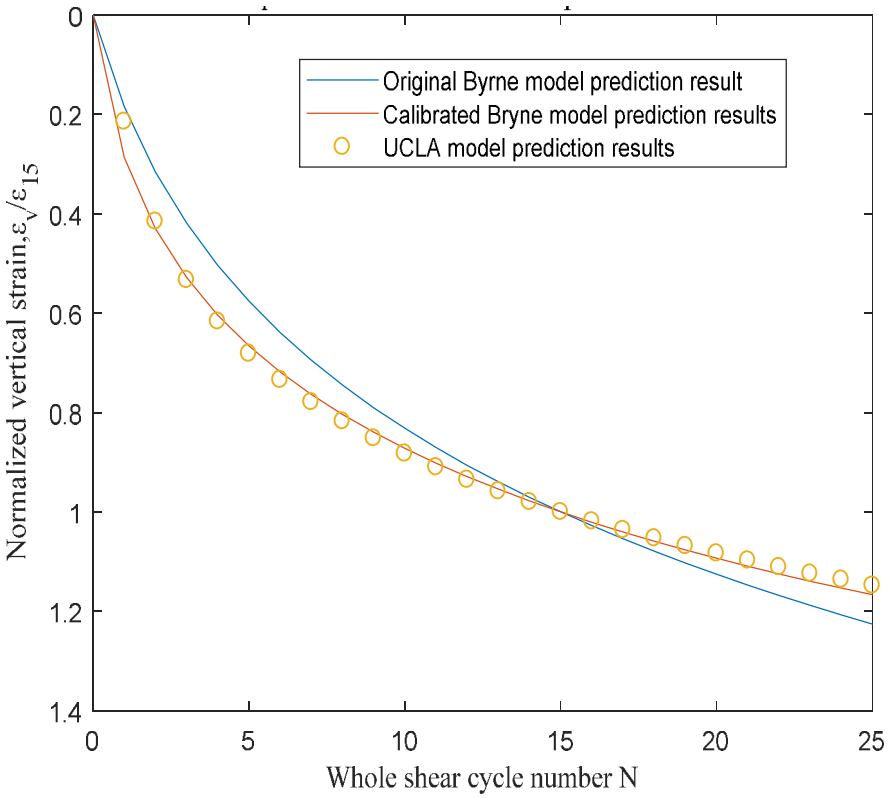

Figure C.7: C_N vs. $n_{eq\gamma}$ prediction comparison among the UCLA model (Duku et al, 2008) with R = 0.29, the Byrne (1991) model with P = 0.4, and the calibrated Byrne model of clean sand with P = 1

Appendix D: MATLAB codes used for model calibration

1. MATLAB functions used to obtain best-fitting C-pair or C-coefficients

1.1 Method 1 used MATLAB function: N_vs_V

The "N_vs_V" is a function code which can be used for processing data of whole cyclic shear cycle N_{whole} vs. accumulated vertical strain ε_v to obtain best-fitting C_1 and C_2. The procedures of conducting curve-fitting by "N_vs_V" were: (1) according to recorded laboratory data of N_{whole} vs. ε_v(%), get column matrix of ε_v (%) and its corresponding column matrix of N_{whole}; (2) import matrixes of N_{whole} and ε_v (%) into MATLAB Workspace window; (3) use script commands or Curve Fitting Toolbox with customized function "N_vs_V" to perform regression. Note that step (3) may need to set the upper and lower limit of C_3, because if the third C_3 value was too large, the regression may not be successfully performed. The inputs and output of this function code were shown in Table D.1

Table D.1: Inputs and output of function code "N_vs_V"

Input	Model coefficients C_1, C_2, and C_3
	Cyclic shear strain magnitude γ (%)
	Threshold shear strain ε_{tv} (%)
	Number of whole shear cycle N_{whole}
Output	Accumulated vertical strain ε_v (%)

The scripts of the code were shown below:

```
function y=N_vs_V(c1,c2,c3,r,rtv,N)
% The output value y is the accumulated vertical strain (%) for any
given whole shear cycle.
% This function has six basic variables:
  % r means shear strain (%) of strain-controlled test.
  % rtv means threshold shear strain (%) of the tested soil.
  % N is the number of whole shear cycle.
  % c1, c2 and c3 are coefficients of Byrne's model.
v(1)=0; % v is the matrix used to store vertical strain values for a
given whole shear cycle. The size of this matrix depends on the
length of N matrix
       % Xxx asign V(1)=0.
r2=(r-rtv)^c3;% r2 is the shear strain related item used for
calculation.
```

```
y = zeros(size(N)); % y is the matrix used to store accumulated
vertical strain for number of whole shear cycles from 0 to N
for j=1:length(N) % In this for loop, length(N) indicates xxx will
use each value (whole shear cycle) of matrix N to do the calculation.
    % The index j is used to mark the order of the N value xxx used
in matrix N
    i=1; % The index xxxxis used to mark the times of iteration
calculation of Byrne's basic model
    while i<=N(j)*2 % In this while loop, N(j)*2 used to represent
the number of half shear cycle for the given value of Matrix N
    deltaX_1(i) = c1*(exp(-c2*(v(i)/r2)))*r2/2;% deltaX_1 is the
volumetric strain increment for every half shear cycle. For the first
cycle, deltaX=C_1*gamma.
    v(i+1)=v(i)+deltaX_1(i);% v is matrix used to store the value of
accumulated vloumetric strain(%)
    i=i+1; % The iteration will end until i= the number of half shear
cycle
    end
y(j)=v(i); % Xxx store the calculated vertical strain (%) for the
given shear cycle into the matrix y, then do the same calculation
once again for next shear cycle that stored in matrix y
% Finally, xxx will get a matrix y which has same size as matrix N
end
end
```

1.2 Method 1 used MATLAB function: N_half_vs_V

The "N_half_vs_V" has same application procedures as function code "N_half_vs_V". But "N_half_vs_V" merely uses half shear cycle N_{half} as input column matrix. The inputs and output of this function code were shown in Table D.2.

Table D.2: Inputs and output of function code "N_half_vs_V"

Input	Model coefficients C_1, C_2, and C_3
	Cyclic shear strain magnitude γ (%)
	Threshold shear strain ε_{tv} (%)
	Number of half shear cycle N_{half}
Output	Accumulated vertical strain ε_v (%)

The scripts of this code were shown below:

```
function y=N_half_vs_V(c1,c2,c3,r,rtv,N)
% The output value y is the accumulated vertical strain (%) for any
given whole shear cycle.
% This function has six basic variables:
  % r means shear strain (%) of strain-controlled test.
  % rtv means threshold shear strain (%) of the tested soil.
  % N is the number of half shear cycle.
  % c1, c2 and c3 are coefficients of Byrne's model.
v(1)=0; % v is the matrix used to store vertical strain values for a
given half shear cycle. The size of this matrix depends on the length
of N matrix
       % Xxx asign V(1)=0.
r2=(r-rtv)^c3;% r2 is the shear strain related item used for
calculation.
y = zeros(size(N)); % y is a matrix used to store accumulated
vertical strain for number of half shear cycles from 0 to N.
for j=1:length(N) % In this for loop, length(N) indicates xxx will
use each values (half shear cycle) of matrix N do the calculation.
    % The index j is used to mark the order of the cyclic shear cycle
xxx used in matrix N.
    i=1;% The index xxxxis used to mark the times of iteration
calculation of Byrne's basic model.
    while i<=N(j) % In this while loop, N(j) used to represent the
number of half shear cycle for the given value of Matrix N.
    deltaX_1(i) = c1*(exp(-c2*(v(i)/r2)))*r2/2;% deltaX_1 is the
volumetric strain increment for every shear cycle. For the first
cycle, deltaX=C_1*gamma.
```

```
    v(i+1)=v(i)+deltaX_1(i);% v is matrix used to store the value of
vloumetric strain(%).
    i=i+1;% The iteration will end until i= the number of half shear
cycle.
    end
y(j)=v(i) % Xxx store the calculated vertical strain (%) for the
given the given shear cycle into the matrix y, then do the same
calculation once again for next the given shear cycle N that stored
in matrix N.
% Finally, xxx will get a matrix y has same size as matrix N.
end
end
```

1.3 Method 2 used MATLAB function: Three_D_fitting

The "Three_D_fitting" is a function code which can be used for processing detailed data of ε_v with its corresponding N_{whole} and γ to obtain best-fitting C_1, C_2, and C_3. The procedures to conducting 3-D curve fitting through MATLAB were shown below: (1) according to recorded data of ε_v(%) with its corresponding N_{whole} and γ (%), obtain same size column matrixes of N_{whole}, ε_v(%), and γ (%); (2) import matrixes of N_{whole}, ε_v(%), and γ (%) into MATLAB workspace area; (3) use script commands or Curve Fitting Toolbox with customized function "Three_D_fitting" to do curve fitting for the imported matrixes of N_{whole}, ε_v(%), and γ (%).Also, it may need to set the C_3 upper and lower limit for step 3. Additionally, it needs to assign specific ε_{tv} value when doing curve fitting. The inputs and output of this function code were shown in Table D.3

Table D.3: Inputs and output of function code "Three_D_fitting"

Input	Model coefficients C_1, C_2, and C_3
	Cyclic shear strain magnitude γ (%)
	Threshold shear strain ε_{tv} (%)
	Number of whole shear cycle N_{whole}
Output	Accumulated vertical strain ε_v (%)

The scripts of this code were shown below:

```
function v=Three_D_fitting(C1,C2,C3,r,rtv,N)
% This function has six basic variables:
  % r means the shear strain (%) of strain-controlled test.
  % rtv means threshold shear strain (%) of the tested soil.
  % N is the considered number of whole shear cycles.
  % c1, c2 and c3 are coefficients of Byrne's model.
% The output value v is the accumulated vertical strain (%) for a
given whole shear cycle N.
if rtv>=r % When the input shear strain is smaller than the threshold
shear strain, xxx assume no volumetric strain occurs.
    v=0;
else
v=zeros(length(r),1);% v is a matrix used to store the accumulated
vertical strain for a given whole shear cycle N
a=-0.5*C1*C2;% a is only a simplified parameter used for calculation
b=length(N); % b is the suites number of the processed data
x = zeros(length(N),1);% x is the a matrix used to store values of
whole shear cycles for each considered test set
slope=zeros(length(N),1);% slope is the a matrix used to store slope
```

```
factor S (It is the calculated result of all items before the item
(r-rtv)^C3)
for j_1=1:b
    r_1(j_1,1)=(r(j_1,1)-rtv)^C3;% For calculation purpose, r_1 is
the substituted parameter for item (r-rtv)^C3
end
for j=1:b % In this for loop, length(x) indicates xxx will use each
values ( whole shear cycle, N) of matrix x to conduct the
calculation.
    % The index j is used to mark the order of the N value xxx used
in matrix x
    ft=zeros(1,1);% ft is the matrix used to store the calculated
t^t...^t(totally 2^2i-1) values when the whole shear cycle is i
    t=exp(a);% Define parameter t
    ft(1,1)=t; % The first item of ft matrix is t
    if N(j)==0 % When the shear cycle is 0
      v(j,1)=0;% When the shear cycle is 0, there is no vertical
strain
    else
for i_1=2:N(j)*2 % Do a for loop calculation, then xxx will get one
item about t^t...^t(totally 2^i_1-1)each time when the half shear
cycle is i_1
ft(i_1,1)=t^t; % Put the calculated t^t...^t into the next index
position
t=t^t;% Do calculation for next index position
end
x(j,1)=prod(ft); % x is the matrix used to store the product of all
calculated t-contained items.
slope(j,1)=-log(x(j,1))/C2 ;% Calculate the slope factor for each
considered whole shear cycle
v(j,1)=slope(j,1)*r_1(j,1); % The arithmetic product of slope factor
and shear strain item is the vertical strain
    end
end
end
end
```

1.4 Method 3 used MATLAB function: N_VS_Nor_V

The "N_VS_Nor_V" is a function code which can be used to process Type 2 data (normalized volumetric strain versus number of cyclic shear cycle) to obtain the C-pair product. The procedures to conducting curve fitting for Type 2 data through MATLAB were shown below: (1) according to recorded data of C_N vs. N_{whole}, obtain same size column matrixes of C_N and N_{whole}; (2) import matrixes of C_N and N_{whole} into MATLAB workspace area; (3) use script commands or Curve Fitting Toolbox with customized function "N_VS_Nor_V" to do curve fitting for the imported column matrixes of C_N and N_{whole}.

At each time after the curve fitting, different best-fitting C_1 and C_2 values will be obtained. That is normal because all these best-fitting C-pair have same product *P*. However, the code "N_VS_Nor_V" can only help us gain the correct value of *P*. The obtained C_1 and C_2 values are not the "true" best-fitting coefficients available for the tested soil. The inputs and output of this function code were shown in Table D.4

Table D.4: Inputs and output of function code "N_VS_Nor_V"

Input	Model coefficients C_1 and C_2
	Cyclic shear strain magnitude γ (%) (can assign random value)
	Number of whole shear cycle N_{whole}
Output	Normalized volumetric strain C_N

The scripts of this code were shown below:

```
function y=N_VS_Nor_V(c1,c2,r,N)
% This function code has four basic variables:
  % r means the shear strain (%) of strain-controlled test.
  % N is the maximum considered number of whole shear cycles.
  % c1 and c2 are coefficients of Byrne's model.
% The output value y is the normalized accumulated vertical strain
(%) for a given whole shear cycle (N) x.
% This function has four basic variables , from which r means gama; x
is the number of shear cycles; c1 and c2 are coefficients for
specific soil.
V(1)=0; % v is the matrix used to store vertical strain values for a
given whole shear cycle. The size of this matrix depends on the
length of N matrix
       % Firstly, xxx assume V(1)=0.
Y = zeros(size(N));%  y is the a matrix used to store normalized
vertical strain for number of whole shear cycles from 0 to N
```

```
t=zeros(size(N));% t is a matrix used to store vertical strain for
each shear cycle
for k=1:30 % Xxx do 30 times calculation, and finally xxx will get
V(31). V(31) is the vertical strain (%) after 15 whole shear cycle.
    % For my code, i-1=the number of half cycle N_half and (i-1)/2 is
the number of whole cycle N_whole when xxxxis odd.
    D=c1*(exp(-c2*(v/r)))*r/2;% d is the volumetric strain increment
for every half shear cycle. For the first cycle, deltaX=C_1*gamma
    v=v+d;% V means accumulated vertical strain
end
w=v % Assign the value of v into w
v(1)=0; % Reassign v(1)=0 for doing another round of iteration.
For j=1:length(N) % In this for loop, length(x) indicates xxx will
use each values ( whole shear cycle, N) of matrix x to do the
calculation.
    % The index j is used to mark the order of the shear cycle value
xxx put in matrix N
    i=1;% The index xxxxis used to direct the times of iteration
calculation of Byrne's basic model
    while i<=N(j)*2 % In this while loop, x(j)*2 means the number of
half shear cycle
    deltaX_1(i) = c1*(exp(-c2*(v(i)/r)))*r/2;% deltaX_1 is the
volumetric strain increment for every shear cycle. For the first
cycle, deltaX=C_1*gamma
    v(i+1)=v(i)+deltaX_1(i);% v is matrix used to store the values of
accumulated 71olumetric strain(%)
    i=i+1; % The iteration will keep running until i= the max number
of whole shear cycle
    end
    t(j)=v(i)% Xxx store the calculated vertical strain (%) for the
given shear cycle into the matrix y, then do the same calculation
once again for next shear cycle that stored in matrix y
% Finally, xxx will get a matrix y which has same size as matrix N
end
y=t/w % Xxx use matrix t over the value of w to get the normalized
volumetric strain stored in matrix y
end
```

2. MATLAB functions of clean sand model and sand with fines of low plasticity model

2.1 Calibrated model of clean sand MATLAB function: Calibrated_clean_sand_ model

The "Calibrated_clean_sand_model" is a function code used for predicting seismic compression magnitude of clean sands. Besides, this code can also be used in case analysis or regressed coefficients checking. In this function, the coefficient expressions were same as presented in Section 2.3.1. The inputs and output of this function code were shown in Table D.5

Table D.5: Inputs and output of function code "Calibrated_clean_sand_model"

Input	Overburden pressure σ_v (kPa)
	Atmosphere pressure Pa usually is 1 (atm)
	Relative density D_r (%)
	Model coefficients C_3
	Cyclic shear strain magnitude γ (%)
	Threshold shear strain ε_{tv} (%)
	Number of whole shear cycle N_{whole}
Output	Accumulated vertical strain ε_v (%)

The scripts of this code were shown below:

```
function v=Calibrated_clean_sand_model(sigma_v,Pa,Dr,C3,r,rtv,N)
% This function has seven basic variables:
  % sigma_v is the vertical load
  % Pa is 1 atm pressure
  % Dr is relative density
  % C3 is the third coefficient of Byrne's model
  % r means shear strain of strain-controlled test.
  % rtv means threshold shear strain of the tested soil.
  % N is the maximum considered number of whole shear cycles.
% The output value y is the accumulated vertical strain (%) for a
given whole shear cycle N.
if rtv>=r
    v=0;
else
C1=(sigma_v/Pa)^(-0.29)*1.92*exp(-0.023*Dr);
C2=1.01/C1;
v=zeros(length(r),1);
a=-0.5*C1*C2;
b=length(N);
```

```
x = zeros(length(N),1);% x is the a matrix used to store values of
whole shear cycles for each considered test set
slope=zeros(length(N),1);% slope is the a matrix used to store slope
factor S which is the calculated result of all items before the shear
strain item (herein refer to r_1=(r-rtv)^C3)
for j_1=1:b
    r_1(j_1,1)=(r(j_1,1)-rtv)^C3;% r_1 is the calibrated shear strain
item used for calculation
end
for j=1:b % In this for loop, length(x) indicates xxx will use each
values ( whole shear cycle, N) of matrix x do the calculation.
    % The index j is used to mark the order of the N value xxx used
in matrix x
    ft=zeros(1,1);% ft is the matrix used to store the calculated
t^t...^t(totally 2^2i-1) values when the whole shear cycle is i
    t=exp(a);% Define parameter t
    ft(1,1)=t; % The first item of ft matrix is t
    if N(j)==0;% When the shear cycle is 0
      v(j,1)=0;% When the shear cycle is 0, there is no vertical
strain
    else
for i_1=2:N(j)*2 ;% Do a for loop calculation,  xxx will get one item
about t^t...^t(totally 2^i_1-1)each time when the half shear cycle is
i_1
ft(i_1,1)=t^t; % Put the calculated t^t...^t into the next index
position
t=t^t;% Do calculation for next index position
end
x(j,1)=prod(ft); % x is the matrix used to store the product of all
calculated t-contained items.
slope(j,1)=-log(x(j,1))/C2 ;% Calculate the slope factor for each
considered whole shear cycle condition
v(j,1)=slope(j,1)*r_1(j,1); % The product of slope factor and shear
strain item is the vertical strain
    end
end
end
end
```

2.2 Calibrated model of sand with fines of low plasticity MATLAB function: Calibrated_sand_with_fine_model

The "Calibrated_sand_with_fine_model" is a function code used for predicting seismic compression magnitude of sand with fines of low plasticity. Besides, this code can also be used in case analysis or regressed coefficients checking. In this function, the coefficient expressions were same as presented in Section 2.3.1. The inputs and output of this function code were shown in Table D.6

Table D.6: Inputs and output of function code "Calibrated_sand_with_fine_model"

Input	Overburden pressure σ_v (kPa)
	Atmosphere pressure Pa (usually assign 1 atm)
	Relative density D_r (%)
	Model coefficients C_3
	Fine content FC (%)
	Degree of saturation S (%)
	Cyclic shear strain magnitude γ (%)
	Threshold shear strain ε_{tv} (%)
	Number of whole shear cycle N_{whole}
Output	Accumulated vertical strain ε_v (%)

The scripts of this code were shown below:

```
function v=Calibrated_sand_with_fine_model(sigma_v,Pa,Dr,FC, S,
C3,r,rtv,N)
% This function has nine basic variables:
  % sigma_v is the vertical load
  % Pa is 1 atm pressure
  % Dr is relative density, in percent
  % FC is the fine content, in percent
  % S is the degree of saturation, in percent
  % C3 is the third coefficient of Byrne's model
  % r means shear strain of strain-controlled test, in percent
  % rtv means threshold shear strain of the tested soil.
  % N is the maximum considered number of whole shear cycles.
% The output value y is the accumulated vertical strain (%) for a
given whole shear cycle N.
if rtv>=r
    v=0;
else
K1=(sigma_v/Pa)^(-0.29); % Overburden pressure correction
% Below are for fine content correction
 if (FC/100)<=0.1
```

```
        K2=1;
    elseif (FC/100)<0.35
            K2=exp(-0.042*(FC-10));
    else
        K2=0.35;
 end
% Below are for degree of saturation correction
      if (FC/100)<=0.1
            K3=1;
       elseif (S/100)<=0.3
            K3=-0.017*S+1;
       elseif (S/100)<=0.5
            K3=0.5;
       elseif (S/100)<=0.6
            K3=0.05*S-2;
       else
            K3=1;
      end
C1=(K1*K2*K3*5.38*exp(-0.023*Dr))/(2.153*r^(-0.2342)+4.341*exp(-
66.57*r));
C2=exp(0.405)*(r-rtv)^0.3291/C1;
v=zeros(length(r),1);
a=-0.5*C1*C2;
b=length(N);
x = zeros(length(N),1);% x is the a matrix used to store values of
whole shear cycles for each considered test set
slope=zeros(length(N),1);% slope is the a matrix used to store slope
factor which is the calculated result of all items before the shear
strain related item (herein refer to r_1=(r-rtv)^C3)
for j_1=1:b
    r_1(j_1,1)=(r(j_1,1)-rtv)^C3;% r_1 is the calibrated shear strain
item used for calculation
end
for j=1:b % In this for loop, length(x) indicates xxx will use each
values ( whole shear cycle, N) of matrix x do the calculation.
    % The index j is used to mark the order of the N value xxx used
in matrix x
    ft=zeros(1,1);% ft is the matrix used to store the calculated
t^t...^t(totally 2^2i-1) values when the whole shear cycle is i
    t=exp(a);% Define parameter t
    ft(1,1)=t; % The first item of ft matrix is t
    if N(j)==0;% When the shear cycle is 0
      v(j,1)=0;% When the shear cycle is 0, there is no vertical
```

```
strain
    else
for i_1=2:N(j)*2 ;% Do a for loop calculation,  xxx will get one item
about t^t...^t(totally 2^i_1-1)each time when the half shear cycle is
i_1
ft(i_1,1)=t^t; % Put the calculated t^t...^t into the next index
position
t=t^t;% Do calculation for next index position
end
x(j,1)=prod(ft); % x is the matrix used to store the product of all
calculated t-contained items.
slope(j,1)=-log(x(j,1))/C2 ;% Calculate the slope factor for each
considered whole shear cycle condition
v(j,1)=slope(j,1)*r_1(j,1); % The product of slope factor and shear
strain item is the vertical strain
    end
end
end
end
```